

Grid-Forming Control with Assignable Voltage Regulation Guarantees and Safety-Critical Current Limiting

Bhathiya Rathnayake and Sijia Geng

Abstract—This paper develops a nonlinear grid-forming (GFM) controller with provable voltage-formation guarantees, with over-current limiting enforced via a control-barrier-function (CBF)-based safety filter. The nominal controller follows a droop-based inner–outer architecture, in which voltage references and frequency are generated by droop laws, an outer-loop voltage controller produces current references using backstepping (BS), and an inner-loop current controller synthesizes the terminal voltage. The grid voltage is treated as an unknown bounded disturbance, without requiring knowledge of its bound, and the controller design does not rely on any network parameters beyond the point of common coupling (PCC). To robustify voltage formation against the grid voltage, a deadzone-adapted disturbance suppression (DADS) framework is incorporated, yielding practical voltage regulation characterized by asymptotic convergence of the PCC voltage errors to an *assignably* small and known residual set. Furthermore, the closed-loop system is proven to be globally well posed, with all physical and adaptive states bounded and voltage error transients (due to initial conditions) decaying exponentially at an assignable rate. On top of the nominal controller, hard over-current protection is achieved through a minimally invasive CBF-based safety filter that enforces strict current limits via a single-constraint quadratic program. The safety filter is compatible with any locally Lipschitz nominal controller. Rigorous analysis establishes forward invariance of the safe-current set and boundedness of all states under current limiting. Numerical results demonstrate improved transient performance and faster recovery during current-limiting events when the proposed DADS-BS controller is used as the nominal control law, compared with conventional PI-based GFM control.

Index Terms—Grid-forming inverters, current limiting, control barrier functions, backstepping, deadzone-adapted disturbance suppression

I. INTRODUCTION

THE electric power system is undergoing a structural transition driven by the large-scale integration of inverter-based resources (IBRs), including solar photovoltaics, battery energy storage systems, and power-electronic-based wind generation. As conventional synchronous generators (SGs) are retired, the grid is gradually losing the electromechanical characteristics that historically provided inertia, frequency support,

and fault current [1]. This transition introduces several challenges: reduced inertia leads to faster and more sensitive frequency dynamics [2]; limited short-circuit current undermines traditional protection schemes [3]; and interactions among inverter controllers can induce complex nonlinear phenomena [4], [5].

Grid-forming (GFM) inverters are widely regarded as vital for future low-inertia power systems due to their capability in directly regulating terminal voltage magnitude and frequency, enabling virtual inertia, frequency regulation, black-start, and robust operation in weak or islanded grids [6]. A large body of work has focused on GFM controllers, including, *droop-based controllers* [7], [8], *virtual synchronous machines* (VSMs) [9]–[11], and *virtual oscillator controllers* (VOCs) with their *dispatchable* (*d*) variants [12]–[15]. Droop control, originating from early microgrid research [16], enforces steady-state active-power–frequency and reactive-power–voltage relationships that enable synchronization and power sharing. VSMs emulate SG dynamics within the inverter controller, while VOCs regulate voltage and frequency through digitally implemented nonlinear oscillators. Despite architectural differences, these GFM controllers present a common external behavior: the inverter acts as a controllable voltage source whose amplitude and frequency vary with reactive and active power, respectively, allowing fast voltage regulation and frequency support.

Unlike SGs, GFM inverters possess limited over-current capability due to semiconductor constraints, typically tolerating only 1.2–2 p.u. current, whereas SGs can, in general, supply 5–7 p.u. current [17]. Consequently, effective current-limiting is critical for device protection during disturbances. Existing approaches are commonly categorized as *direct* or *indirect* methods [3]. Direct methods, such as current-reference saturation [18], [19] and switch-level limiting [20], [21], enforce current bounds accurately but may compromise voltage-source behavior and post-fault recovery. Indirect methods—including virtual impedance [22], [23] and voltage-based limiting [24], [25]—better preserve voltage-source characteristics but generally lack guarantees of hard current bounds. Constraint-aware voltage shaping methods have also been proposed to indirectly limit current through feasibility projections or optimization [26], [27]. More recently, *control barrier function* (CBF)-based approaches have emerged as a systematic framework for enforcing safety constraints in control systems [28] and power systems [29]. In the GFM context, CBF-based current limiters [30], [31] explicitly impose hard current bounds through online

This work was supported by the Ralph O’Connor Sustainable Energy Institute (ROSEI) at Johns Hopkins University. Corresponding Author: Sijia Geng.

B. Rathnayake is with the Ralph O’Connor Sustainable Energy Institute (ROSEI), Johns Hopkins University, Baltimore, MD, USA (email: brathna1@jh.edu).

S. Geng is with the Department of Electrical and Computer Engineering, Johns Hopkins University, Baltimore, MD, USA (email: sgeng@jhu.edu).

optimization, typically via a *quadratic program (QP)*, while minimally modifying a nominal voltage-forming controller.

Despite these advances, several challenges remain. First, many representative GFM controllers across different architectures [9]–[11], [16], [32] rely on proportional–integral–derivative (PID) control or variants applied to inherently nonlinear inverter dynamics. In such designs, theoretical guarantees are typically established separately from controller synthesis. While model-based nonlinear designs aim to more explicitly link control laws with guarantees, many existing approaches [33]–[35] assume accurate network models, require observers or estimators, or rely on higher-order derivatives of electrical measurements, which can be difficult to obtain and tune in practice. Second, the systematic integration of hard over-current protection into GFM controllers remains largely unresolved. Current limiting is often implemented using heuristic mechanisms [3], [17], and it is unclear whether such mechanisms can be non-trivially incorporated into existing GFM control architectures. Although CBFs provide a principled tool for embedding current constraints, only a limited number of works [29]–[31] have explored this direction for GFM inverters.

To address such issues, this paper develops a droop-based, backstepping (BS) GFM controller for grid-connected IBRs. The grid voltage is treated as an unknown bounded disturbance, without requiring knowledge of the bound. Furthermore, the design requires no knowledge of network parameters beyond the point of common coupling (PCC).

To robustify the voltage-forming objective against the grid voltage, we tailor the recently introduced *deadzone-adapted disturbance suppression (DADS)* framework [36]–[38] to the inverter dq-channel dynamics and the active/reactive power filters. DADS combines (i) a deadzone in the adaptive law for a controller gain—activating adaptation only when a suitable error-energy measure is above a prescribed threshold, thereby preventing gain drift—with (ii) dynamic nonlinear damping terms that inject additional dissipation. This structure yields disturbance suppression that asymptotically regulates the relevant states to an *assignably small and known* residual set in the presence of unknown but constant network parameters and bounded disturbances of arbitrarily large magnitude.

On top of the nominal voltage-forming controller, we incorporate a QP-based safety filter that enforces a hard bound on the inverter terminal current via a CBF constraint. The filter is minimally invasive: it modifies the nominal terminal-voltage command only when necessary to prevent current-limit violations, thereby preserving GFM behavior as closely as possible within the safe region.

The contributions of this work are summarized as follows.

1) *Nominal Droop-based BS GFM controller with DADS (DADS-BS) (Section III)*: We propose a nonlinear GFM controller with an inner–outer architecture in which the frequency and PCC voltage references are generated by active/reactive power droop with second-order power filters. The outer-loop voltage controller produces reference currents that act as *virtual* controls in BS, while the inner-loop current controller synthesizes the terminal-voltage inputs and incorporates the DADS framework. The design requires no knowledge of

network parameters beyond the PCC and employs neither disturbance observers nor parameter estimators.

2) *Global well-posedness and boundedness under bounded disturbances (Theorem 1)*: For the nominal DADS-BS (without current limiting), we establish global existence and uniqueness of solutions and boundedness of *all* closed-loop states—the PCC voltage, inverter and grid currents, power-filter states, and DADS adaptive gains. The closed-loop system satisfies the bounded-input bounded-state property with respect to the bounded grid voltage.

3) *Transient performance and asymptotic voltage-formation guarantees (Theorem 2)*: We show that convergence of the PCC voltage errors to a region determined by unknown constant network parameters and grid voltage bounds is *exponential* with an *assignable* convergence rate. Moreover, we establish practical voltage regulation: the PCC voltage asymptotically tracks the droop-generated reference within a *designer-specified* residual neighborhood, independently of the disturbance magnitude and unknown constant network parameters. These guarantees remain valid even under severe fault conditions, such as three-phase-to-ground faults at the grid. Explicit tradeoffs among residual size, adaptation rates, and control effort are discussed.

4) *Hard over-current protection with closed-loop boundedness guarantees (Theorems 4 and 5)*: We enforce strict terminal-current limits using a CBF-based safety filter that minimally modifies the nominal terminal-voltage command through a single-constraint QP. A closed-form expression for the safety-filtered control is obtained, eliminating the need for online QP solvers. For arbitrary locally Lipschitz nominal controllers filtered through this safety filter, we prove forward invariance of the safe-current set and boundedness of all remaining physical states. Specializing to the proposed DADS-BS, we further analyze the interaction between current-limiting events and adaptive dynamics, and establish boundedness of the adaptive gains under a mild activation-pattern assumption on the safety filter (finite number and total duration of ON intervals). Numerical results demonstrate improved transient behavior and recovery of nominal GFM behavior during current-limiting events when using DADS-BS as the nominal controller, compared with standard PI-based GFM control.

Notation. $\mathbb{R}_+ := [0, +\infty)$ and $\mathbb{R}_{>0} := (0, +\infty)$. For a vector $\mathbf{x} \in \mathbb{R}^{n_1}$, $\|\mathbf{x}\|$ denotes its Euclidean norm, and for $x \in \mathbb{R}$, $|x| = \|x\|$. Let $D \subset \mathbb{R}^{n_1}$ be an open set and let $S \subset \mathbb{R}^{n_1}$ be a set that satisfies $D \subseteq S \subseteq \text{cl}(D)$, where $\text{cl}(D)$ is the closure of D . By $C^0(S; \Omega)$, we denote the class of continuous functions on S , which take values in $\Omega \subseteq \mathbb{R}^{n_2}$. Let the non-empty set $\Theta \subset \mathbb{R}^{n_3}$ be given. By $L^\infty(\mathbb{R}_+; \Theta)$ we denote the class of essentially bounded, Lebesgue measurable functions $\mathbf{d} : \mathbb{R}_+ \rightarrow \Theta$. For $\mathbf{d} \in L^\infty(\mathbb{R}_+; \Theta)$, we define $\|\mathbf{d}\|_\infty := \sup_{t \geq 0} (\|\mathbf{d}(t)\|)$, where $\sup_{t \geq 0} (\|\mathbf{d}(t)\|)$ is the essential supremum. By \mathcal{K} , we denote the class of increasing continuous functions $\alpha : \mathbb{R}_+ \rightarrow \mathbb{R}_+$ with $\alpha(0) = 0$.

The paper is organized as follows. Section II presents generic modeling of grid-connected IBRs. Section III introduces the DADS-BS framework for droop-based GFM control. Section IV proposes a CBF-based QP safety filter for enforcing strict terminal-current constraints. Section V presents

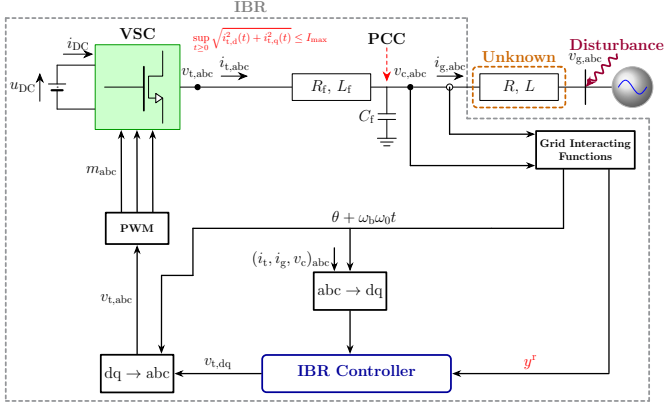


Fig. 1: An IBR connected to the grid. In GFL operation, the objective is to inject prescribed active and reactive power at the PCC; in GFM operation, the objective is to establish the voltage waveform at the PCC.

numerical simulations. Section VI provides the proofs of all theoretical results presented in Sections III and IV. Section VII concludes the paper.

II. MODELING OF GRID-CONNECTED IBRS

A. Reference Frames and Coordinate Transformations

Figure 1 shows a three-phase voltage source converter (VSC) connected to the grid through an output filter and a transmission line. The inverter synthesizes terminal voltages $v_{t,abc} := (v_{t,a}, v_{t,b}, v_{t,c})$, which drive terminal currents $i_{t,abc} := (i_{t,a}, i_{t,b}, i_{t,c})$. The point of common coupling (PCC) voltages are denoted by $v_{c,abc} := (v_{c,a}, v_{c,b}, v_{c,c})$, and the currents by $i_{g,abc} := (i_{g,a}, i_{g,b}, i_{g,c})$. The grid-side voltages are $v_{g,abc} := (v_{g,a}, v_{g,b}, v_{g,c})$.

Although abc variables provide a direct physical description, they remain sinusoidal and time-varying even under steady-state balanced conditions, which complicates analysis and control design. Reference-frame transformations are therefore employed to express these quantities in rotating coordinates, where steady-state signals appear constant.

Following standard practice in IBR modeling [5], [8], we use two reference frames: a *global* rotating DQ frame for network-level modeling and stability analysis, and *local* rotating dq frames attached to individual inverters for control design and implementation.

Each inverter operates in a local dq frame rotating at angular velocity $\omega \omega_b$ rad/s, where ω is the per-unit electrical frequency and ω_b is the base electrical angular frequency (e.g., $\omega_b = 2\pi \times 60$ rad/s). Under balanced three-phase operation, any set of abc variables can be mapped without loss of information to two components, d and q , via the Park transformation (see [39]). A global rotating DQ frame is introduced to provide a unified coordinate system for the network. This frame rotates at angular velocity $\omega_{DQ} \omega_b$ rad/s and is typically chosen such that $\omega_{DQ} = \omega_0$, the steady-state grid frequency, so that electrical quantities are constant at equilibrium. Figure 2 shows the PCC voltage expressed in both

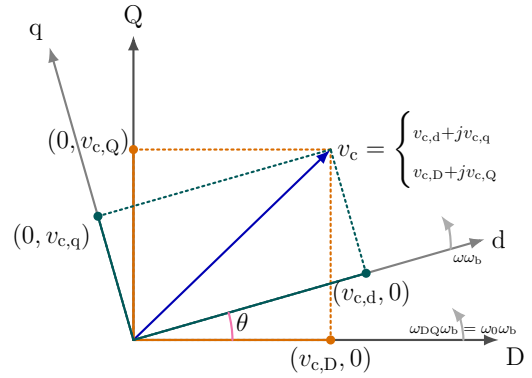


Fig. 2: PCC voltage in the dq and DQ frames.

frames. In the local dq frame, the PCC voltage is represented as the complex quantity

$$v_c = v_{c,d} + jv_{c,q},$$

while in the global DQ frame it is given by

$$v_c = v_{c,D} + jv_{c,Q}.$$

All other voltages and currents are represented analogously.

Let θ denote the angular displacement of the local dq frame relative to the global DQ frame, as illustrated in Fig. 2. The evolution of this angle satisfies

$$\dot{\theta} = \omega_b(\omega - \omega_0),$$

capturing the relative frequency deviation between the frames.

The transformation between the dq and DQ coordinates is given by the *invertible* rotation matrix

$$\mathbf{R}(\theta) := \begin{bmatrix} \cos \theta & -\sin \theta \\ \sin \theta & \cos \theta \end{bmatrix},$$

so that, for example, the PCC voltage components satisfy

$$\begin{bmatrix} v_{c,D} \\ v_{c,Q} \end{bmatrix} = \mathbf{R}(\theta) \begin{bmatrix} v_{c,d} \\ v_{c,q} \end{bmatrix}.$$

Transformations for all other quantities follow analogously. In the single-inverter infinite-bus setting considered below, all inverter states and control laws are expressed in the local dq frame. The grid voltage is assumed bounded; hence, no explicit DQ–dq transformation is required in the analysis. Such a transformation is only used in simulations to convert the DQ grid voltage into the local dq frame.

Assumption 1. *The DC-side dynamics are neglected, with the DC-link voltage u_{DC} assumed constant and the DC current i_{DC} determined algebraically to supply the required power. PWM switching dynamics are assumed sufficiently fast so that the inverter terminal voltages track their commanded dq setpoints instantaneously. The transmission line is modeled by lumped series resistance and inductance.*

B. Circuit Dynamics

The d and q channel circuit dynamics of an IBR connected to the grid, as shown in Fig. 1, are given by

$$\dot{v}_{c,d} = \omega_b \omega v_{c,q} + \frac{\omega_b}{C_f} (i_{t,d} - i_{g,d}), \quad (1)$$

$$\dot{v}_{c,q} = -\omega_b \omega v_{c,d} + \frac{\omega_b}{C_f} (i_{t,q} - i_{g,q}), \quad (2)$$

$$\dot{i}_{t,d} = \omega_b \omega i_{t,q} + \frac{\omega_b}{L_f} (v_{t,d} - v_{c,d}) - \frac{\omega_b R_f}{L_f} i_{t,d}, \quad (3)$$

$$\dot{i}_{t,q} = -\omega_b \omega i_{t,d} + \frac{\omega_b}{L_f} (v_{t,q} - v_{c,q}) - \frac{\omega_b R_f}{L_f} i_{t,q}, \quad (4)$$

$$\dot{i}_{g,d} = \omega_b \omega i_{g,q} + \frac{\omega_b}{L} (v_{c,d} - v_{g,d}) - \frac{\omega_b R}{L} i_{g,d}, \quad (5)$$

$$\dot{i}_{g,q} = -\omega_b \omega i_{g,d} + \frac{\omega_b}{L} (v_{c,q} - v_{g,q}) - \frac{\omega_b R}{L} i_{g,q}. \quad (6)$$

See Appendix A of [8] for a derivation of IBR dynamics in a rotating reference frame.

Define the inverter electrical state vector

$$\mathbf{x}_{\text{inv}} := [v_{c,d}, v_{c,q}, i_{t,d}, i_{t,q}, i_{g,d}, i_{g,q}]^\top \in \mathbb{R}^6,$$

with initial condition $\mathbf{x}_{\text{inv}}(0) \in \mathbb{R}^6$. The signals $v_{t,d}, v_{t,q}$ respectively denote the d- and q-axis control inputs, to be specified by an inner controller. The signals $v_{g,d}, v_{g,q}$ represent the d- and q-components of the grid voltage. The electrical frequency ω is locked to the grid in GFL operation, for example via a PLL, whereas in GFM operation, it is autonomously generated by the inverter, for example, using droop. For notational convenience, we collect the constant physical parameters into

$$\boldsymbol{\Omega} := [\omega_b, C_f, L_f, R_f, L, R]^\top \in \mathbb{R}_{>0}^6. \quad (7)$$

The network parameters $R, L > 0$ belong to the external network (see Fig. 1) and are typically unknown to the inverter control design *a priori* or subject to uncertainty. Therefore, throughout the analysis, we treat R and L as unknown but positive constants. No knowledge of R or L is required for the controller design.

Assumption 2. *The grid voltage $v_g = v_{g,d} + jv_{g,q}$ is a bounded signal such that*

$$v_{g,d}, v_{g,q} \in L^\infty(\mathbb{R}_+; \mathbb{R}).$$

Although we assume that the grid voltage is bounded, no numerical upper bound is used in the controller design.

In practical implementations, a hard current magnitude constraint $\sqrt{i_{g,d}^2(t) + i_{g,q}^2(t)} \leq I_{\text{max}}$ for all $t \geq 0$ must be enforced to reflect semiconductor and thermal limits. This constraint will be explicitly enforced through the proposed safety-critical control design discussed in Section IV.

III. GRID-FORMING INVERTER CONTROL

This section presents a nonlinear GFM controller obtained by integrating droop laws with a deadzone-adapted disturbance suppression (DADS)-type backstepping (BS) design. The primary objectives are: 1) to regulate the PCC voltage components $(v_{c,d}, v_{c,q})$ to the droop-generated references $(v_{c,d}^r, v_{c,q}^r)$,

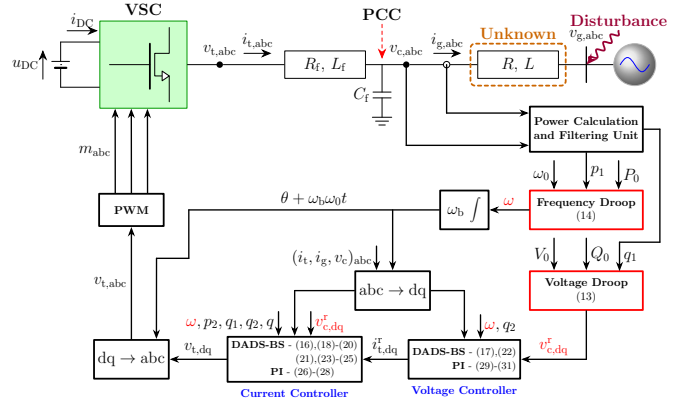


Fig. 3: Droop-based GFM control architecture with DADS-BS or PI lower-level control loops.

and 2) to ensure boundedness of all closed-loop states, including terminal and grid currents, the power filter states, and the adaptive gains. The proposed controller achieves these objectives despite the presence of unknown but bounded grid voltage and unknown constant network parameters $R, L > 0$. All control laws are designed in the local dq reference frame. Current limiting on i_t is not considered in this section, and will be addressed in Section IV.

A. Droop Relationships

We first define the instantaneous active and reactive powers at the PCC as

$$p = v_{c,d} i_{g,d} + v_{c,q} i_{g,q}, \quad (8)$$

$$q = v_{c,q} i_{g,d} - v_{c,d} i_{g,q}. \quad (9)$$

The instantaneous powers (p, q) are passed through second-order low-pass filters with saturation. Specifically, the filtered reactive and active powers evolve according to

$$\dot{q}_1 = q_2, \quad \dot{q}_2 = -2\xi_q \omega_{qc} q_2 - \omega_{qc}^2 (q_1 - \text{sat}_{\bar{Q}}(q)), \quad (10)$$

$$\dot{p}_1 = p_2, \quad \dot{p}_2 = -2\xi_p \omega_{pc} p_2 - \omega_{pc}^2 (p_1 - \text{sat}_{\bar{P}}(p)), \quad (11)$$

with initial conditions $q_1(0), q_2(0), p_1(0), p_2(0) \in \mathbb{R}$. The filter parameters satisfy $\xi_q, \xi_p > 1$ and $\omega_{qc}, \omega_{pc} > 0$, while $\bar{Q}, \bar{P} \in (0, +\infty]$ denote saturation thresholds. The saturation function $\text{sat}_{\bar{x}}: \mathbb{R} \rightarrow \mathbb{R}$ with $\bar{x} \in (0, +\infty]$ is defined as

$$\text{sat}_{\bar{x}}(y) := \begin{cases} \bar{x}, & y > \bar{x}, \\ y, & -\bar{x} \leq y \leq \bar{x}, \\ -\bar{x}, & y < -\bar{x}. \end{cases} \quad (12)$$

Based on the filtered powers (p_1, q_1) , the GFM voltage reference and frequency are generated via droop relationships. In particular, the reactive-power-voltage droop law is

$$v_{c,d}^r = V_0 + K_Q(Q_0 - q_1), \quad v_{c,q}^r \equiv 0, \quad (13)$$

while the active-power-frequency droop law is given by

$$\omega = \omega_0 + K_P(P_0 - p_1). \quad (14)$$

Here, $V_0, \omega_0 \in \mathbb{R}$ denote nominal voltage magnitude and frequency in p.u., $K_Q, K_P \in \mathbb{R}$ are droop gains in p.u.,

and $P_0, Q_0 \in \mathbb{R}$ are active- and reactive-power setpoints in p.u. The references $(v_{c,d}^r, v_{c,q}^r)$ are then tracked by an inner-loop controller, which generates the terminal voltage inputs $(v_{t,d}, v_{t,q})$. Figure 3 shows the droop-based control architecture considered below.

We collect the inverter electrical states \mathbf{x}_{inv} and the power-filter states into the augmented state vector

$$\mathbf{x} := [\mathbf{x}_{\text{inv}}, q_1, q_2, p_1, p_2]^\top \in \mathbb{R}^{10}. \quad (15)$$

Remark 1. The inclusion of the saturation operator in the reactive-power–voltage droop channel is instrumental for ensuring bounded droop-generated voltage references and for capturing the physical limitations of GFM inverters. In particular, the droop law (13) must generate bounded voltage references; without saturation, the voltage reference may become unbounded under large reactive-power deviations. In practice, GFM inverters have finite apparent-power ratings and voltage levels, and exceeding these limits can lead to thermal overstress and malfunction of semiconductor devices and violations of grid codes. The operator $\text{sat}_{\overline{Q}}(\cdot)$ therefore provides a safe and physically meaningful operating envelope for the reactive-power–voltage droop.

From a theoretical standpoint, a saturation operator on the active-power–frequency droop is not required for the boundedness claims (Theorem 1) or the performance guarantees (Theorem 2). One may therefore set $\overline{P} = +\infty$ without affecting the analysis. Imposing saturation solely on the reactive-power–voltage channel is sufficient, since it enforces boundedness of the droop-generated voltage reference, which—together with the controller introduced below—yields bounded closed-loop behavior, including the electrical frequency.

B. DADS-BS Control Laws

The proposed controller follows a typical inner-outer loop control architecture. The PCC voltage dynamics are shaped by introducing reference terminal currents $i_{t,d}^r$ and $i_{t,q}^r$, which act as *virtual control inputs* in backstepping (BS) and serve as *outer-loop voltage controllers*. The actual control inputs, namely the terminal voltages $v_{t,d}$ and $v_{t,q}$, are then designed to track these reference currents while canceling matched nonlinearities, thereby serving as *inner-loop current controllers*.

To robustify the design against disturbances, the BS controller is augmented with DADS-type nonlinear damping terms containing dynamically adapted gains z_d and z_q . In particular, the dynamic gains modulate the damping injection and are updated through deadzone-based adaptation laws.

We now present the resulting control laws.

d-axis Control Law

$$\begin{aligned} v_{t,d} = \frac{L_f}{\omega_b} & \left[-2\omega_b\omega(i_{t,q} - i_{g,q}) + \frac{\omega_b R_f}{L_f} i_{t,d} \right. \\ & + \omega_b \left(\frac{1}{L_f} + \omega^2 C_f \right) v_{c,d} + C_f K_P p_2 v_{c,q} \\ & - K_{VC} (i_{t,d} - i_{t,d}^r) + \frac{C_f K_{VC}^2}{\omega_b} (v_{c,d} - v_{c,d}^r) \\ & + \frac{2\xi_q \omega_{qc} K_Q C_f}{\omega_b} q_2 + \frac{\omega_{qc}^2 K_Q C_f}{\omega_b} (q_1 - \text{sat}_{\overline{Q}}(q)) \\ & \left. + u_d \right], \quad K_{VC} > 0, \end{aligned} \quad (16)$$

$$i_{t,d}^r = i_{g,d} - C_f \omega v_{c,q} - \frac{C_f K_Q}{\omega_b} q_2 - \frac{C_f K_{VC}}{\omega_b} (v_{c,d} - v_{c,d}^r), \quad (17)$$

$$\begin{aligned} u_d = - & \left(K_{CC} + \frac{(1 + e^{z_d}) \omega_b^2}{4\mu_d} (1 + i_{g,d}^2 + v_{c,d}^2) \right) (i_{t,d} - i_{t,d}^r) \\ & - \frac{\omega_b}{C_f} (v_{c,d} - v_{c,d}^r), \quad K_{CC}, \mu_d > 0, \end{aligned} \quad (18)$$

$$\dot{z}_d = \Gamma_d e^{-z_d} \max \{ W_d - \varepsilon, 0 \}, \quad \Gamma_d, \varepsilon > 0, \quad (19)$$

$$W_d = \frac{1}{2} (v_{c,d} - v_{c,d}^r)^2 + \frac{1}{2} (i_{t,d} - i_{t,d}^r)^2. \quad (20)$$

q-axis Control Law

$$\begin{aligned} v_{t,q} = \frac{L_f}{\omega_b} & \left[2\omega_b\omega(i_{t,d} - i_{g,d}) + \frac{\omega_b R_f}{L_f} i_{t,q} \right. \\ & + \omega_b \left(\frac{1}{L_f} + C_f \omega^2 + \frac{C_f K_{VC}^2}{\omega_b^2} \right) v_{c,q} - C_f K_P p_2 v_{c,d} \\ & \left. - K_{VC} (i_{t,q} - i_{t,q}^r) + u_q \right], \quad K_{VC} > 0, \end{aligned} \quad (21)$$

$$i_{t,q}^r = i_{g,q} + C_f \omega v_{c,d} - \frac{C_f K_{VC}}{\omega_b} v_{c,q}, \quad (22)$$

$$\begin{aligned} u_q = - & \left(K_{CC} + \frac{(1 + e^{z_q}) \omega_b^2}{4\mu_q} (1 + i_{g,q}^2 + v_{c,q}^2) \right) (i_{t,q} - i_{t,q}^r) \\ & - \frac{\omega_b}{C_f} v_{c,q}, \quad K_{CC}, \mu_q > 0, \end{aligned} \quad (23)$$

$$\dot{z}_q = \Gamma_q e^{-z_q} \max \{ W_q - \varepsilon, 0 \}, \quad \Gamma_q, \varepsilon > 0, \quad (24)$$

$$W_q = \frac{1}{2} v_{c,q}^2 + \frac{1}{2} (i_{t,q} - i_{t,q}^r)^2. \quad (25)$$

Equations (17) and (22) serve as outer voltage controllers whereas (16),(18)-(20) and (21),(23)-(25) serve as inner current controllers. The auxiliary inputs u_d and u_q inject nonlinear damping and implement the DADS mechanism. The gains $K_{VC} > 0$ and $K_{CC} > 0$ are respectively the voltage and current control gains. The parameters $\mu_d, \mu_q > 0$ tune the strength of the nonlinear damping injection and determine the trade-off between control effort and disturbance attenuation (c.f. (34),(35)). The adaptive gains z_d, z_q with dynamics (19), (24) compensate for unknown bounded grid voltage and

unknown network parameters $R, L > 0$. The adaptation rates $\Gamma_d, \Gamma_q > 0$ determine the speed of gain adjustment.

The DADS-BS controller (16)–(25) combines classical BS with nonlinear dynamic damping, adaptation of the gains z_d and z_q , and a deadzone mechanism. The nonlinear damping terms $\frac{(1+e^{z_\ell})\omega_b^2}{4\mu_\ell}$, $\ell \in \{d, q\}$, provide disturbance suppression without requiring prior bounds on disturbance magnitude or knowledge of network parameters $R, L > 0$. The deadzone in (19),(24) ensures that adaptation is activated only when the energy signals W_d and W_q are above a user-specified threshold $\varepsilon > 0$, and frozen otherwise, thereby preventing gain drift and guaranteeing their boundedness.

Remark 2. For reference, a classical PI-based GFM controller [5] is given below. The controller consists of a voltage controller that generates reference terminal currents and a current controller that computes the terminal voltages.

Current controller (inner loop):

$$v_{t,d} = -K_{CC}^P(i_{t,d} - i_{t,d}^r) - K_{CC}^I\gamma_d + K_{CC}^F v_{c,d} - \omega L_f i_{t,q}, \quad (26)$$

$$v_{t,q} = -K_{CC}^P(i_{t,q} - i_{t,q}^r) - K_{CC}^I\gamma_q + K_{CC}^F v_{c,q} + \omega L_f i_{t,d}, \quad (27)$$

with integral states

$$\dot{\gamma}_d = i_{t,d} - i_{t,d}^r, \quad \dot{\gamma}_q = i_{t,q} - i_{t,q}^r. \quad (28)$$

Voltage controller (outer loop):

$$i_{t,d}^r = -K_{VC}^P(v_{c,d} - v_{c,d}^r) - K_{VC}^I\beta_d + K_{VC}^F i_{g,d} - \omega C_f v_{c,q}, \quad (29)$$

$$i_{t,q}^r = -K_{VC}^P(v_{c,q} - v_{c,q}^r) - K_{VC}^I\beta_q + K_{VC}^F i_{g,q} + \omega C_f v_{c,d}, \quad (30)$$

with integral states

$$\dot{\beta}_d = v_{c,d} - v_{c,d}^r, \quad \dot{\beta}_q = v_{c,q}. \quad (31)$$

The DADS-BS preserves this voltage and current control architecture and thus, can be integrated into existing PI-based GFM control stacks without major modifications; see Fig. 3.

C. Boundedness of States and Performance Guarantees

We establish the assignable voltage regulation guarantees in this subsection, including the boundedness of states and performance guarantees.

Firstly, the DADS-BS controller ensures boundedness of all closed-loop states (c.f. (32),(33)) in the presence of bounded grid disturbances, i.e., the closed-loop system exhibits a bounded-input bounded-state (BIBS) property for each fixed parameter vector $\Omega \in \mathbb{R}_{>0}^6$ defined in (7). No claim of uniformity with respect to the parameters—particularly the unknown network parameters $R, L > 0$ —is made.

Theorem 1 (Boundedness of states). Consider the droop-based GFM inverter described by (1)-(15). Fix design parameters $K_{VC}, K_{CC}, \mu_d, \mu_q, \Gamma_d, \Gamma_q, \varepsilon, \omega_{pc}, \omega_{qc}, \bar{Q} > 0, \bar{P} \in (0, +\infty]$, and $\xi_p, \xi_q > 1$. Let the setpoints $\omega_0, V_0, P_0, Q_0 \in \mathbb{R}$ and the droop coefficients $K_P, K_Q \in \mathbb{R}$ be given. Choose the control inputs $v_{t,d}$ and $v_{t,q}$ according to (16)-(20) and (21)-(25), respectively. Assume the grid voltage components satisfy $v_{g,d}, v_{g,q} \in L^\infty(\mathbb{R}_+; \mathbb{R})$. Then, for each fixed $\Omega \in \mathbb{R}_{>0}^6$ defined in (7), there exists a function $B_{1,\Omega} \in C^0(\mathbb{R}^{10} \times \mathbb{R} \times$

$\mathbb{R} \times \mathbb{R}_+ \times \mathbb{R}_+; \mathbb{R}_+)$, such that, for every $(\mathbf{x}(0), z_d(0), z_q(0)) \in \mathbb{R}^{10} \times \mathbb{R} \times \mathbb{R}$, the unique absolutely continuous solution of (1)-(25) exists, and satisfies the following estimates for all $t \geq 0$:

$$\|\mathbf{x}(t)\| \leq B_{1,\Omega}(\mathbf{x}(0), z_d(0), z_q(0), \|v_{g,d}\|_\infty, \|v_{g,q}\|_\infty), \quad (32)$$

and

$$\begin{aligned} z_\ell(0) \leq z_\ell(t) &\leq \lim_{s \rightarrow \infty} z_\ell(s) \\ &\leq B_{1,\Omega}(\mathbf{x}(0), z_d(0), z_q(0), \|v_{g,d}\|_\infty, \|v_{g,q}\|_\infty), \end{aligned} \quad (33)$$

where $\ell \in \{d, q\}$.

The proof for Theorem 1 is provided in Section VI-B.

Secondly, we prove that the DADS-BS can regulate the PCC voltage errors into arbitrarily small residual sets of size $\sqrt{2\varepsilon}$ (c.f. (37),(38)), independently of grid disturbances and unknown constant network parameters $R, L > 0$. This is achieved because the adaptive gains z_d and z_q are pumped up as needed to counteract disturbances and uncertainties, i.e., sufficient adaptation is provided through the gain dynamics. The explicit upper bound on $z_\ell, \ell = \{d, q\}$ in (33) is $\ln \left(\max \left\{ \frac{\mu_\ell(1+R^2+\|v_{g,\ell}\|_\infty^2)}{2kL^2\varepsilon} - 1, e^{z_\ell(0)} \right\} + \frac{\Gamma_\ell}{2k} \max \left\{ W_\ell(0) + \frac{\mu_\ell(1+R^2+\|v_{g,\ell}\|_\infty^2)}{2kL^2(1+e^{z_\ell(0)})} - \varepsilon, 0 \right\} \right)$, (see the proof of Theorem 1). This shows that the upper bound on z_ℓ necessarily increases as $\varepsilon > 0$ decreases, reflecting the increased adaptation required to drive the PCC voltage errors into smaller desired regions.

Furthermore, the convergence of the PCC voltage components to the regions $|v_{c,d}(t) - v_{c,d}^r| \leq \left(\frac{\mu_d(1+R^2+\|v_{g,d}\|_\infty^2)}{kL^2} \right)^{1/2}$ and $|v_{c,q}| \leq \left(\frac{\mu_q(1+R^2+\|v_{g,q}\|_\infty^2)}{kL^2} \right)^{1/2}$ (c.f. the decay estimates (34),(35)) is exponential with decay rate k tunable via $K_{VC}, K_{CC} > 0$. Convergence to the ultimate residual sets $|v_{c,d} - v_{c,d}^r| \leq \sqrt{2\varepsilon}$ and $|v_{c,q}| \leq \sqrt{2\varepsilon}$ may be slower, but can be accelerated by increasing the adaptation gains Γ_d, Γ_q at the cost of increased control effort.

Theorem 2 (Performance guarantees). Consider the droop-based GFM inverter described by (1)-(15). Fix design parameters $K_{VC}, K_{CC}, \mu_d, \mu_q, \Gamma_d, \Gamma_q, \varepsilon, \omega_{pc}, \omega_{qc}, \bar{Q} > 0, \bar{P} \in (0, +\infty]$, and $\xi_p, \xi_q > 1$. Let the setpoints $\omega_0, V_0, P_0, Q_0 \in \mathbb{R}$ and the droop coefficients $K_P, K_Q \in \mathbb{R}$ be given. Choose the control inputs $v_{t,d}$ and $v_{t,q}$ according to (16)-(20) and (21)-(25), respectively. Assume the grid voltage components satisfy $v_{g,d}, v_{g,q} \in L^\infty(\mathbb{R}_+; \mathbb{R})$ and that the network parameters $R, L > 0$ are unknown but constant. For any initial condition $(\mathbf{x}(0), z_d(0), z_q(0)) \in \mathbb{R}^{10} \times \mathbb{R} \times \mathbb{R}$, let $t \mapsto (\mathbf{x}(t), z_d(t), z_q(t))$ denote the corresponding unique absolutely continuous closed-loop solution on $[0, \infty)$. Then, the following estimates hold for all $t \geq 0$:

$$\begin{aligned} (v_{c,d}(t) - v_{c,d}^r(t))^2 &\leq 2W_d(t) \leq 2e^{-2kt}W_d(0) + \frac{\mu_d(1+R^2+\|v_{g,d}\|_\infty^2)}{kL^2}, \end{aligned} \quad (34)$$

$$v_{c,q}^2(t) \leq 2W_q(t) \leq 2e^{-2kt}W_q(0) + \frac{\mu_q(1+R^2+\|v_{g,q}\|_\infty^2)}{kL^2}, \quad (35)$$

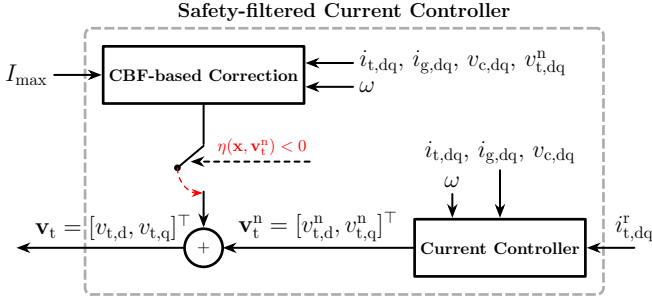


Fig. 4: CBF-based safety filtering of the current controller. The CBF correction is activated when $\eta(\mathbf{x}, \mathbf{v}_t^n) < 0$; see (45).

where $k > 0$ is

$$k = \min\{K_{VC}, K_{CC}\}. \quad (36)$$

Moreover,

$$\limsup_{t \rightarrow +\infty} (|v_{c,d}(t) - v_{c,d}^r(t)|) \leq \sqrt{2\varepsilon}, \quad (37)$$

$$\limsup_{t \rightarrow +\infty} (|v_{c,q}(t)|) \leq \sqrt{2\varepsilon}. \quad (38)$$

The proof for Theorem 2 is provided in Section VI-C.

Remark 3. The performance guarantees (34)-(38) remain valid even under severe fault conditions, such as three-phase-to-ground faults at the grid, *i.e.*, $\sqrt{v_{g,d}^2(t) + v_{g,q}^2(t)} \equiv 0$. Indeed, such faulted grid voltages still belong to $L^\infty(\mathbb{R}_+; \mathbb{R})$, which is the only assumption imposed on the grid voltage signals in the analysis.

IV. OVER-CURRENT LIMITING WITH CONTROL BARRIER FUNCTIONS

In this section, we address the problem of enforcing hard current limits on the inverter terminal current. To this end, we incorporate a CBF based safety filter that admits an arbitrary locally Lipschitz nominal controller and guarantees that the magnitude of the inverter terminal current, $i_t = i_{t,d} + j i_{t,q}$, does not exceed a prescribed bound I_{\max} . The proposed construction is independent of the specific nominal controller and therefore applies, in particular, to the proposed DADS-BS controller. Figure 4 illustrates the CBF-based modification to the current controller module in Fig. 3, ensuring that the terminal-current magnitude remains below I_{\max} . We first briefly review the CBF framework, then specialize it to the terminal-current dynamics of the GFM inverter, and finally establish forward invariance of the safe-current set together with boundedness of the remaining closed-loop states. We also address the issue of boundedness of the adaptive gains (z_d, z_q) when the nominal controller is chosen as DADS-BS.

A. Safety-critical control with locally Lipschitz nominal controllers

Definition 1 (Extended class \mathcal{K} functions). A continuous function $\alpha : [-a_0, a_1] \rightarrow [-\infty, \infty)$, $a_0 > 0, a_1 > 0$ belongs to extended class \mathcal{K} if it is strictly increasing and $\alpha(0) = 0$.

We consider a general nonlinear control-affine system of the form

$$\dot{\mathbf{y}} = \mathbf{f}(\mathbf{y}) + \mathbf{g}(\mathbf{y})\mathbf{u}, \quad (39)$$

where $\mathbf{f} : \mathbb{R}^n \rightarrow \mathbb{R}^n$ and $\mathbf{g} : \mathbb{R}^n \rightarrow \mathbb{R}^{n \times m}$ are smooth maps, $\mathbf{y} \in \mathbb{R}^n$ is the state, and $\mathbf{u} \in \mathbb{R}^m$ is the control input.

Definition 2 (Forward invariant set). A set $\mathcal{C}_y \subseteq \mathbb{R}^n$ is forward invariant for system (39) if every solution with initial condition $\mathbf{y}(0) \in \mathcal{C}_y$ satisfies $\mathbf{y}(t) \in \mathcal{C}_y$ for all $t \geq 0$.

Definition 3 (Control barrier function [28]). Let

$$\mathcal{C}_y := \{\mathbf{y} \in \mathbb{R}^n : h(\mathbf{y}) \geq 0\},$$

for a continuously differentiable function $h : \mathbb{R}^n \rightarrow \mathbb{R}$. The function h is a control barrier function (CBF) for system (39) on \mathcal{C}_y if there exists an extended class \mathcal{K} function α such that

$$\sup_{\mathbf{u}} [L_{\mathbf{f}}h(\mathbf{y}) + L_{\mathbf{g}}h(\mathbf{y})\mathbf{u} + \alpha(h(\mathbf{y}))] \geq 0, \quad \forall \mathbf{y} \in \mathcal{C}_y,$$

and $L_{\mathbf{g}}h(\mathbf{y}) \neq 0$ whenever $h(\mathbf{y}) = 0$. Here, $L_{\mathbf{f}}$ and $L_{\mathbf{g}}$ denote the Lie derivatives along \mathbf{f} and \mathbf{g} , respectively.

Theorem 3 ([28]). Suppose h is a CBF for (39) on \mathcal{C}_y . Let α be the associated extended class \mathcal{K} function. If a locally Lipschitz feedback law $\mathbf{u} = \mathbf{k}(\mathbf{y})$ with $\mathbf{k} : \mathbb{R}^n \rightarrow \mathbb{R}^m$ satisfies

$$\dot{h}(\mathbf{y}, \mathbf{u}) \geq -\alpha(h(\mathbf{y})), \quad \forall \mathbf{y} \in \mathcal{C}_y,$$

then the set \mathcal{C}_y is forward invariant for the closed-loop system.

We now apply the above framework to the terminal-current dynamics of the droop-based GFM inverter. Concatenating the current dynamics (3),(4), we obtain

$$\dot{\mathbf{i}}_t = \mathbf{A}(\mathbf{x})\mathbf{i}_t - \frac{\omega_b}{L_f}\mathbf{v}_c + \frac{\omega_b}{L_f}\mathbf{v}_t,$$

where

$$\mathbf{i}_t := \begin{bmatrix} i_{t,d} \\ i_{t,q} \end{bmatrix}, \quad \mathbf{v}_c := \begin{bmatrix} v_{c,d} \\ v_{c,q} \end{bmatrix}, \quad \mathbf{v}_t := \begin{bmatrix} v_{t,d} \\ v_{t,q} \end{bmatrix},$$

and

$$\mathbf{A}(\mathbf{x}) = \begin{bmatrix} -\frac{R_f}{L_f}\omega_b & \omega_b\omega \\ -\omega_b\omega & -\frac{R_f}{L_f}\omega_b \end{bmatrix}.$$

Here, \mathbf{x} denotes the state vector given by (15).

We enforce the constraint that the magnitude of the terminal current is bounded by $I_{\max} > 0$, that is,

$$\|\mathbf{i}_t\|^2 = i_{t,d}^2 + i_{t,q}^2 \leq I_{\max}^2.$$

This defines the safe set

$$\mathcal{C} := \{\mathbf{x} \in \mathbb{R}^{10} | i_{t,d}^2 + i_{t,q}^2 \leq I_{\max}^2\}. \quad (40)$$

To encode this requirement as a CBF condition, we introduce the barrier function

$$h(\mathbf{x}) := I_{\max}^2 - i_{t,d}^2 - i_{t,q}^2 = I_{\max}^2 - \mathbf{i}_t^\top \mathbf{i}_t. \quad (41)$$

Differentiating h along the trajectories of the system yields

$$\begin{aligned} \dot{h}(\mathbf{x}) &= -2\mathbf{i}_t^\top \dot{\mathbf{i}}_t \\ &= -2\mathbf{i}_t^\top \mathbf{A}(\mathbf{x})\mathbf{i}_t + \frac{2\omega_b}{L_f}\mathbf{i}_t^\top \mathbf{v}_c - \frac{2\omega_b}{L_f}\mathbf{i}_t^\top \mathbf{v}_t. \end{aligned}$$

Since \dot{h} depends affinely on \mathbf{v}_t , we can enforce a CBF inequality of the form

$$\dot{h}(\mathbf{x}) \geq -c h(\mathbf{x}), \quad (42)$$

for some design constant $c > 0$, by constraining \mathbf{v}_t .

Let the nominal control be denoted by

$$\mathbf{v}_t^n = \begin{bmatrix} v_{t,d}^n \\ v_{t,q}^n \end{bmatrix}.$$

This nominal control may be any locally Lipschitz function of the state. We then construct a safety filter that modifies \mathbf{v}_t^n only as needed to satisfy (42). To this end, we solve the quadratic program (QP)

$$\begin{aligned} \min_{\mathbf{v}_t} \quad & \|\mathbf{v}_t - \mathbf{v}_t^n\|^2 \\ \text{s.t.} \quad & -2\mathbf{i}_t^\top \mathbf{A}(\mathbf{x})\mathbf{i}_t + \frac{2\omega_b}{L_f} \mathbf{i}_t^\top \mathbf{v}_c - \frac{2\omega_b}{L_f} \mathbf{i}_t^\top \mathbf{v}_t \geq -c h(\mathbf{x}), \end{aligned} \quad (43)$$

which explicitly enforces the CBF condition with $\alpha(s) = cs$. The problem (43) is strictly convex with a single affine inequality constraint and thus admits a unique optimal solution.

Define

$$\eta(\mathbf{x}, \mathbf{v}_t^n) := -2\mathbf{i}_t^\top \mathbf{A}(\mathbf{x})\mathbf{i}_t + \frac{2\omega_b}{L_f} \mathbf{i}_t^\top \mathbf{v}_c - \frac{2\omega_b}{L_f} \mathbf{i}_t^\top \mathbf{v}_t^n + c h(\mathbf{x}). \quad (44)$$

The nominal control \mathbf{v}_t^n satisfies the constraint in (43) if and only if $\eta(\mathbf{x}, \mathbf{v}_t^n) \geq 0$. Otherwise, the constraint is violated, in which case, the optimal solution of (43) is given by the projection of \mathbf{v}_t^n onto the half-space defined by the affine constraint. This results in the explicit solution

$$\mathbf{v}_t = \begin{cases} \mathbf{v}_t^n, & \eta(\mathbf{x}, \mathbf{v}_t^n) \geq 0, \\ \mathbf{v}_t^n + \frac{L_f}{2\omega_b} \frac{\eta(\mathbf{x}, \mathbf{v}_t^n)}{\|\mathbf{i}_t\|^2} \mathbf{i}_t, & \text{otherwise.} \end{cases} \quad (45)$$

See Fig. 4 also. When $\|\mathbf{i}_t\| = 0$, the CBF constraint in (43) reduces to $0 \geq -cI_{\max}^2$, which is trivially satisfied since $I_{\max}^2 > 0$. Thus, when $\mathbf{i}_t = 0$, the CBF condition imposes no restriction on \mathbf{v}_t , and therefore the nominal control \mathbf{v}_t^n is applied without modification.

Below, for the ease of stating results, we collect the states excluding terminal current components $(i_{t,d}, i_{t,q})$ into \mathbf{x}' as

$$\mathbf{x}' := [v_{c,d}, v_{c,q}, i_{g,d}, i_{g,q}, q_1, q_2, p_1, p_2]^\top \in \mathbb{R}^8. \quad (46)$$

Theorem 4 (Safety with locally Lipschitz nominal controllers). *Consider the droop-based GFM inverter described by (1)-(15). Fix design parameters $\omega_{pc}, \omega_{qc} > 0$, $\xi_p, \xi_q > 1$, and $\bar{P}, \bar{Q} \in (0, +\infty]$. Let the setpoints $\omega_0, V_0, P_0, Q_0 \in \mathbb{R}$, the droop coefficients $K_P, K_Q \in \mathbb{R}$, and the maximum allowable terminal current $I_{\max} > 0$ be given. Let the current-limiting barrier function $h(\mathbf{x}) : \mathbb{R}^{10} \rightarrow \mathbb{R}$ be given by (41). Suppose the terminal-voltage control $\mathbf{v}_t = [v_{t,d}, v_{t,q}]^\top$ is implemented according to (44),(45), for an arbitrary locally Lipschitz nominal control $\mathbf{v}_t^n = \mathbf{k}(\mathbf{x})$, with $\mathbf{k} : \mathbb{R}^{10} \rightarrow \mathbb{R}^2$. Assume the grid voltage components satisfy $v_{g,d}, v_{g,q} \in L^\infty(\mathbb{R}_+; \mathbb{R})$. Then, for every initial condition $\mathbf{x}(0) \in \mathcal{C}$, with \mathcal{C} defined*

in (40), the closed-loop system admits a unique absolutely continuous solution for all $t \geq 0$, and

$$\sqrt{i_{t,d}^2(t) + i_{t,q}^2(t)} \leq I_{\max}, \quad (47)$$

all $t \geq 0$. Moreover, for each fixed $\Omega \in \mathbb{R}_{>0}^6$ defined in (7), there exists a function $B_{2,\Omega} \in C^0(\mathbb{R}^{10} \times \mathbb{R}_+ \times \mathbb{R}_+)$, such that

$$\|\mathbf{x}'(t)\| \leq B_{2,\Omega}(\mathbf{x}(0), \|v_{g,d}\|_\infty, \|v_{g,q}\|_\infty), \quad (48)$$

for all $t \geq 0$, where \mathbf{x}' is given by (46).

The proof for Theorem 4 is provided in Section VI-D.

B. Safe DADS-BS GFM control

We now specialize to the case where the nominal controller \mathbf{v}_t^n is chosen as the DADS-BS.

Proposition 1. *Consider the droop-based GFM inverter described by (1)-(15). Fix design parameters $K_{VC}, K_{CC}, \mu_d, \mu_q, \Gamma_d, \Gamma_q, \varepsilon, \omega_{pc}, \omega_{qc} > 0$, $\xi_p, \xi_q > 1$, and $\bar{P}, \bar{Q} \in (0, +\infty]$. Let the setpoints $\omega_0, V_0, P_0, Q_0 \in \mathbb{R}$, the droop coefficients $K_P, K_Q \in \mathbb{R}$, and the maximum allowable terminal current $I_{\max} > 0$ be given. Let the current-limiting barrier function $h(\mathbf{x}) : \mathbb{R}^{10} \rightarrow \mathbb{R}$ be given by (41). Suppose the terminal-voltage control $\mathbf{v}_t = [v_{t,d}, v_{t,q}]^\top$ is implemented according to (44),(45), where the nominal control $\mathbf{v}_t^n = [v_{t,d}^n, v_{t,q}^n]^\top$ is the DADS-BS defined in (16)-(25). Assume the grid voltage components satisfy $v_{g,d}, v_{g,q} \in L^\infty(\mathbb{R}_+; \mathbb{R})$. Then, for each fixed $\Omega \in \mathbb{R}_{>0}^6$ defined in (7) and for every initial condition $\mathbf{x}(0) \in \mathcal{C}$ (with \mathcal{C} defined in (40)) and $z_d(0), z_q(0) \in \mathbb{R}$, the closed-loop system admits a unique absolutely continuous solution for all $t \geq 0$.*

The proof for Proposition 1 is provided in Section VI-E.

To show explicitly that the adaptive gains z_d and z_q are bounded under the safety-filtered DADS-BS control, we analyze the activation pattern of the safety filter.

For a given solution $t \mapsto (\mathbf{x}(t), z_d(t), z_q(t))$ of the safety-filtered DADS-BS closed-loop system (1)-(25),(44),(45) define

$$\eta(t) := \eta(\mathbf{x}(t), \mathbf{v}_t^n(t)). \quad (49)$$

Since $\mathbf{x}(\cdot)$ and $\mathbf{v}_t^n(\cdot)$ are continuous and the map $(\mathbf{x}, \mathbf{v}_t^n) \mapsto \eta(\mathbf{x}, \mathbf{v}_t^n)$ is locally Lipschitz, it follows that $\eta(\cdot)$ is continuous on \mathbb{R}_+ .

We define the ON set

$$\mathcal{I}_{\text{on}} := \{t \geq 0 \mid \eta(t) < 0\},$$

that is, the set of times at which the safety filter is active and the implemented control differs from the nominal one. If $\eta(0) < 0$, then there exists $\sigma_0 > 0$ such that $[0, \sigma_0) \subset \mathcal{I}_{\text{on}}$. After this possible initial ON interval, all remaining ON episodes are ordinary open intervals, because $\eta(\cdot)$ is continuous. Thus \mathcal{I}_{on} can be decomposed as

$$\mathcal{I}_{\text{on}} = ([0, \sigma_0) \text{ if } \eta(0) < 0) \cup \bigcup_{\kappa \in \mathcal{J}} (\tau_\kappa, \sigma_\kappa), \quad (50)$$

where $\mathcal{J} \subseteq \mathbb{N}$ (possibly empty) and each interval $(\tau_\kappa, \sigma_\kappa)$ satisfies $0 < \tau_\kappa < \sigma_\kappa \leq +\infty$. Each interval in (50) is interpreted as one ON episode of the safety filter: at $t = \tau_\kappa$ the filter turns ON (i.e., η becomes negative), for $t \in (\tau_\kappa, \sigma_\kappa)$ it remains ON, and at $t = \sigma_\kappa$ it turns OFF when $\eta(t)$ returns to 0.

We define the number of ON episodes and the total ON time by

$$N_\eta := \begin{cases} 1 + \text{card}(\mathcal{J}), & \text{if } \eta(0) < 0, \\ \text{card}(\mathcal{J}), & \text{if } \eta(0) \geq 0, \end{cases} \quad (51)$$

$$T_\eta := \begin{cases} \sigma_0 + \sum_{\kappa \in \mathcal{J}} (\sigma_\kappa - \tau_\kappa), & \text{if } \eta(0) < 0, \\ \sum_{\kappa \in \mathcal{J}} (\sigma_\kappa - \tau_\kappa), & \text{if } \eta(0) \geq 0, \end{cases} \quad (52)$$

so that N_η counts all ON episodes and T_η gives their total length. Here, $\text{card}(\cdot)$ denotes the cardinality of a set.

Assumption 3. For every initial condition $\mathbf{x}(0) \in \mathcal{C}$ and $z_d(0), z_q(0) \in \mathbb{R}$, and for every bounded grid voltage $v_{g,d}, v_{g,q} \in L^\infty(\mathbb{R}_+; \mathbb{R})$, consider the corresponding closed-loop solution of (1)-(25),(45),(44) and define N_η and T_η by (51),(52). Then, for each fixed $\Omega \in \mathbb{R}_{>0}^6$ defined in (7), there exist $N_\Omega \in \mathbb{N}$ and $T_\Omega \in (0, \infty)$ possibly depending on $\mathbf{x}(0), z_d(0), z_q(0), \|v_{g,d}\|_\infty, \|v_{g,q}\|_\infty$, such that

$$N_\eta \leq N_\Omega, \quad T_\eta \leq T_\Omega.$$

Assumption 3 states that, along any closed-loop trajectory with $\mathbf{x}(0) \in \mathcal{C}$, $z_d(0), z_q(0) \in \mathbb{R}$ and $v_{g,d}, v_{g,q} \in L^\infty(\mathbb{R}_+; \mathbb{R})$, the safety filter is activated only finitely many times and that the total duration of safety-filter activation is finite.

Remark 4. Assumption 3 imposes two constraints on the set \mathcal{I}_{on} of safety-filter ON times. First, $N_\eta \leq N_\Omega < \infty$ implies that \mathcal{I}_{on} consists of at most N_Ω disjoint ON intervals: possibly an initial interval $[0, \sigma_0)$ if $\eta(0) < 0$, followed by the intervals $(\tau_\kappa, \sigma_\kappa)$, $\kappa \in \mathcal{J}$. Since $T_\eta \leq T_\Omega < \infty$, each of these intervals has finite length, and therefore every right-endpoint σ_0 (if present) and σ_κ satisfies $\sigma_0 < +\infty$, $\sigma_\kappa < +\infty$, $\kappa \in \mathcal{J}$.

Hence, the set of all right-endpoints,

$$\Sigma := \{\sigma_0 \text{ if } \eta(0) < 0\} \cup \{\sigma_\kappa \mid \kappa \in \mathcal{J}\},$$

is finite and possibly empty, and we define

$$\sigma_{\max} := \sup(\Sigma),$$

with the convention $\sup \emptyset := 0$, so that $\sigma_{\max} < +\infty$. For all $t \geq \sigma_{\max}$ we therefore have $t \notin \mathcal{I}_{\text{on}}$, or equivalently,

$$t \geq \sigma_{\max} \implies \eta(t) \geq 0.$$

Thus, under Assumption 3, the safety filter can be activated only finitely many times, and there exists a finite time after which it remains permanently OFF. In particular, if the safety filter is never activated (i.e., $\mathcal{I}_{\text{on}} = \emptyset$), then $\sigma_{\max} = 0$.

Below we establish the main results under the safety-filtered DADS-BS control.

Theorem 5 (Safety with DADS-BS nominal controller). Consider the droop-based GFM inverter described by (1)-(15). Fix design parameters $K_{\text{VC}}, K_{\text{CC}}, \mu_d, \mu_q, \Gamma_d, \Gamma_q, \varepsilon, \omega_{\text{pc}}, \omega_{\text{qc}} > 0$, $\xi_p, \xi_q > 1$, and $\bar{P}, \bar{Q} \in (0, +\infty]$. Let the setpoints $\omega_0, V_0, P_0, Q_0 \in \mathbb{R}$, the droop coefficients $K_P, K_Q \in \mathbb{R}$, and the maximum allowable terminal current $I_{\max} > 0$ be given. Let the current-limiting barrier function $h(\mathbf{x}) : \mathbb{R}^{10} \rightarrow \mathbb{R}$ be given by (41). Suppose the terminal-voltage control $\mathbf{v}_t = [v_{t,d}, v_{t,q}]^\top$ is implemented according to (44),(45) where the nominal control $\mathbf{v}_t^n = [v_{t,d}^n, v_{t,q}^n]^\top$ is the DADS-BS defined

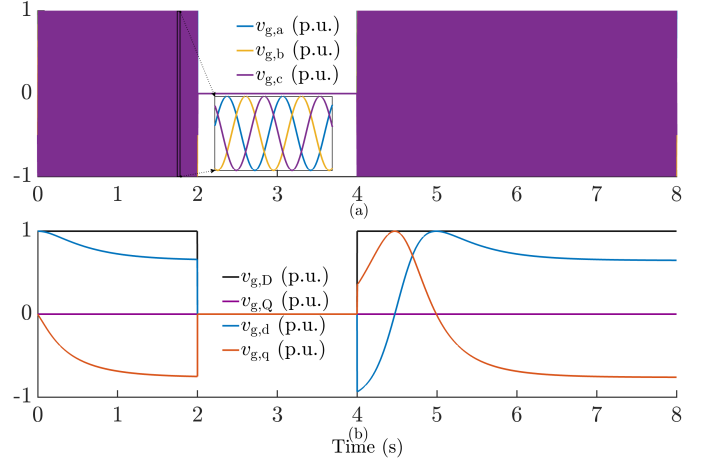


Fig. 5: Grid voltage. A three-phase-to-ground fault occurs from $t = 2$ s to $t = 4$ s. (a) Three-phase voltages. (b) Global dq and local dq components.

in (16)-(25). Assume the grid voltage components satisfy $v_{g,d}, v_{g,q} \in L^\infty(\mathbb{R}_+; \mathbb{R})$. For each fixed $\Omega \in \mathbb{R}_{>0}^6$ defined in (7) and any initial condition $\mathbf{x}(0) \in \mathcal{C}$ (with \mathcal{C} defined in (40)) and $z_d(0), z_q(0) \in \mathbb{R}$, let $t \mapsto (\mathbf{x}(t), z_d(t), z_q(t))$ denote the unique absolutely continuous closed-loop solution on $[0, \infty)$. Then the solution satisfies (47) and (48) for all $t \geq 0$. Moreover, subject to Assumption 3, there exists a function $B_{3,\Omega} : \mathbb{R}^{10} \times \mathbb{R} \times \mathbb{R} \times \mathbb{R}_+ \times \mathbb{R}_+ \times \mathbb{N} \times \mathbb{R}_+ \rightarrow \mathbb{R}_+$, such that for each $\ell \in \{d, q\}$, the adaptive gains satisfy

$$z_\ell(0) \leq z_\ell(t) \leq \lim_{s \rightarrow \infty} z_\ell(s) \leq B_{3,\Omega}(\mathbf{x}(0), z_d(0), z_q(0), \|v_{g,d}\|_\infty, \|v_{g,q}\|_\infty, N_\Omega, T_\Omega), \quad (53)$$

for all $t \geq 0$.

The proof for Theorem 5 is provided in Section VI-F.

Remark 5. Unlike in Theorems 1 and 2, in Theorems 4 and 5 we allow both $\bar{P}, \bar{Q} \in (0, +\infty]$. This is because the CBF-QP safety filter enforces the hard constraint $\|\dot{\mathbf{i}}_t\| \leq I_{\max}$ for all time, which prevents terminal-current blow-up regardless of whether the power-filter inputs are saturated. As a consequence, the remaining electrical states are bounded under the safety-filtered control, and saturation of the reactive- and active-power inputs in (10),(11) is not required for the boundedness conclusions of Theorems 4 and 5.

V. NUMERICAL RESULTS

This section evaluates the proposed DADS-BS GFM controller against a conventional cascaded PI voltage-current control architecture [5], both **without** and **with** the proposed current-limiting mechanism. Specifically, we report two comparisons: (i) DADS-BS versus PI with the safety filter disabled (i.e., DADS-BS and PI are applied for all times without considering safety), and (ii) Safe DADS-BS versus Safe PI with the safety filter enabled, that is, using DADS-BS and PI as nominal controllers within the safety-filtered control law in (44),(45). The PI controller structure and tuned following [5].

The inverter and network parameters are selected in p.u. as $C_f = 0.30$, $L_f = 0.05$, $R_f = 7.2 \times 10^{-3}$, $R = 0.2$, $L = 0.8$,

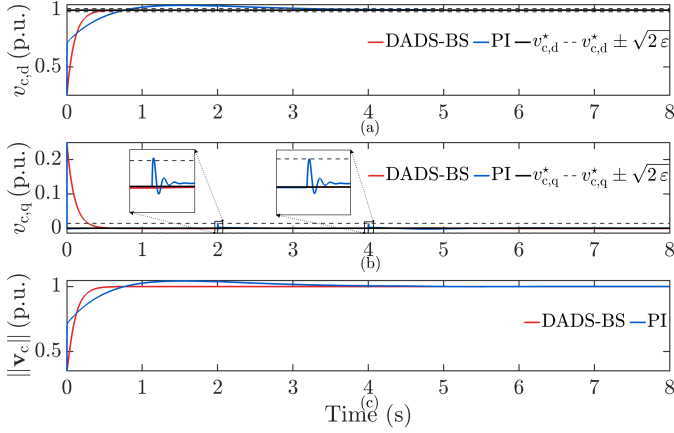


Fig. 6: PCC voltage behavior **without** current limiting. (a) d component. (b) q component. (c) $v_c = \sqrt{v_{c,d}^2 + v_{c,q}^2}$.

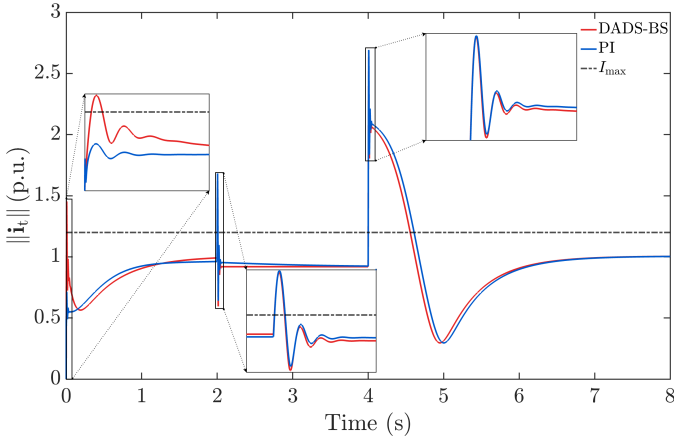


Fig. 7: Terminal current behavior **without** current limiting.

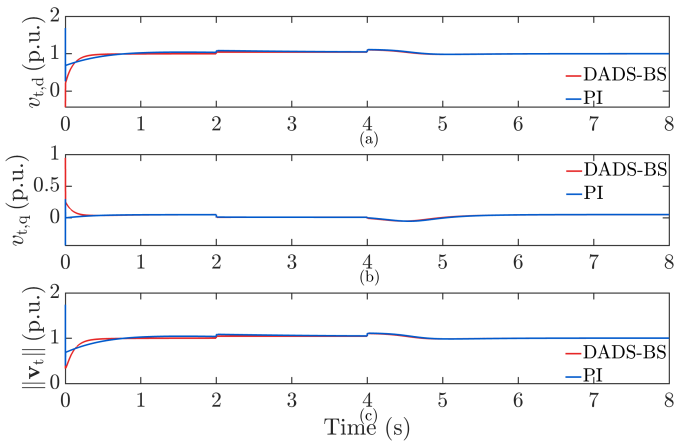


Fig. 8: Terminal voltage (control input) **without** current limiting. (a) d component. (b) q component. (c) $v_t = \sqrt{v_{t,d}^2 + v_{t,q}^2}$.

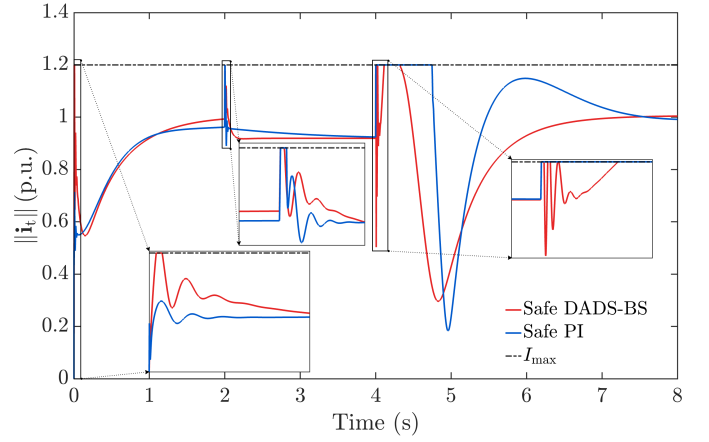


Fig. 9: Terminal current behavior **with** current limiting.

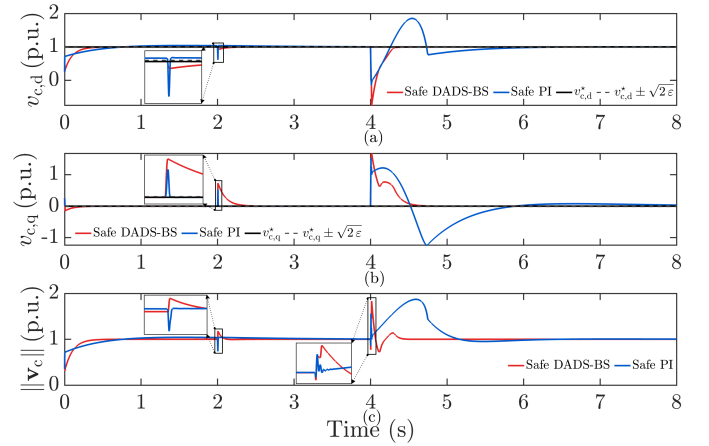


Fig. 10: PCC voltage behavior **with** current limiting. (a) d component. (b) q component. (c) $v_c = \sqrt{v_{c,d}^2 + v_{c,q}^2}$.

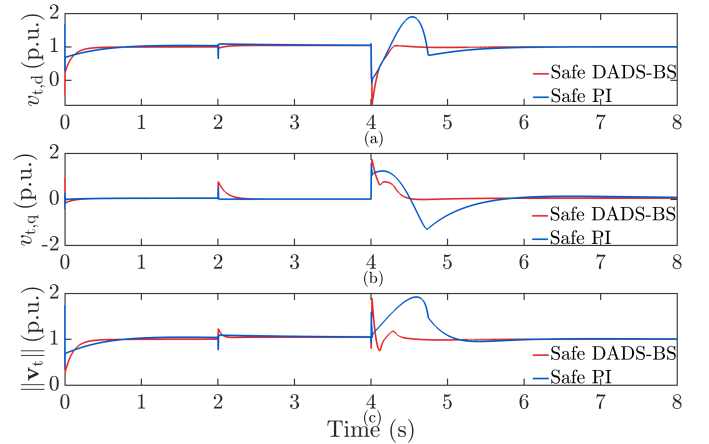


Fig. 11: Terminal voltage (control input) **with** current limiting. (a) d component. (b) q component. (c) $v_t = \sqrt{v_{t,d}^2 + v_{t,q}^2}$.

and the base electrical frequency as $\omega_b = 120\pi$ rad/s. For the DADS-BS controller, the gains and adaptive-law parameters are $K_{VC} = K_{CC} = 10\text{ s}^{-1}$, $\Gamma_d = \Gamma_q = 10^6\text{ s}^{-1}$, $\mu_d = \mu_q = 1\text{ s}^{-1}$, $\varepsilon = 10^{-4}$. The droop parameters and setpoints are chosen in p.u. as $K_P = 5 \times 10^{-3}$, $K_Q = 1 \times 10^{-4}$, $P_0 = 1$, $Q_0 = 0.5$, $\omega_0 = 1$, $V_0 = 1$, and the power filter parameters are chosen as $\omega_{pc} = 332.8\text{ rad/s}$, $\omega_{qc} = 732.8\text{ rad/s}$, $\xi_p = 1.2$, $\xi_q = 1.2$. The simulations use the same initial conditions across all cases. For current limiting, the bound is set to $I_{\max} = 1.2$ p.u., and the safety-filter gain is chosen as $c = 1 \times 10^9\text{ s}^{-1}$. All simulations are performed using a stiff solver (MATLAB `ode15s`) with tolerances `RelTol` = 10^{-7} , `AbsTol` = 10^{-9} , and `MaxStep` = 10^{-4} .

Figure 5 shows the grid voltage, with Fig. 5(a) depicting the three-phase abc voltages and Fig. 5(b) showing the grid voltage in the global DQ frame. During $t \in [2, 4]$ s, a three-phase-to-ground fault is applied at the grid.

Figures 6–8 present the results **without** current limiting for both DADS-BS and PI control. As shown in Fig. 6, variations in the grid voltage do not affect DADS-BS due to its disturbance-suppression property, and convergence within the $\sqrt{2\varepsilon}$ bands is observed, as guaranteed by the theory. However, Fig. 7 shows that both DADS-BS and PI exceed the allowable terminal current limit $I_{\max} = 1.2$, primarily triggered by the fault, highlighting the necessity of explicit current-limiting mechanisms. Figure 8 shows the terminal voltages (control inputs) under both DADS-BS and PI.

Figures 9–11 show the results **with** current limiting for both Safe DADS-BS and Safe PI. As seen in Fig. 9, both controllers effectively enforce the current limit without violation. However, as a consequence, Fig. 10 shows that both Safe DADS-BS and Safe PI temporarily deviate from their GFM objectives. This behavior reflects an inherent tradeoff between strict enforcement of hard current constraints and voltage regulation. When the safety constraint becomes active, the controller prioritizes current limitation, thereby temporarily relaxing voltage regulation. This deviation arises because the admissible control set is restricted by the CBF constraint during current-limiting events. Notably, Safe DADS-BS recovers rapidly during and after the fault and promptly resumes GFM behavior, demonstrating superior transient performance during and following current-limiting events. Figure 11 shows the terminal voltages under both Safe DADS-BS and Safe PI.

VI. PROOFS

A. Auxiliary Lemmas

Lemma 1. *Let $b > 0$, $\xi > 1$, and let $u \in L^\infty(\mathbb{R}_+; \mathbb{R})$ with $\|u\|_\infty = M$. Consider the system*

$$\dot{\eta}_1 = \eta_2, \quad (54)$$

$$\dot{\eta}_2 = -2\xi b \eta_2(t) - b^2 \eta_1 + b^2 u, \quad (55)$$

for $t \geq 0$, with initial condition $(\eta_1(0), \eta_2(0)) = (\eta_{10}, \eta_{20}) \in \mathbb{R}^2$. Then, there exists a unique absolutely continuous solution

$(\eta_1, \eta_2) : \mathbb{R}_+ \rightarrow \mathbb{R}^2$ to (54), (55), and it satisfies

$$|\eta_1(t)| \leq \frac{\xi|\eta_{10}| + \frac{|\eta_{20}|}{b}}{\sqrt{\xi^2 - 1}} + M, \quad (56)$$

$$|\eta_2(t)| \leq \frac{b|\eta_{10}| + \xi|\eta_{20}|}{\sqrt{\xi^2 - 1}} + \frac{bM}{\sqrt{\xi^2 - 1}}, \quad (57)$$

for all $t \geq 0$.

Proof. We rewrite the system in vector form as

$$\dot{\eta} = \mathbf{H}\eta + \mathbf{B}u,$$

where

$$\eta = \begin{bmatrix} \eta_1 \\ \eta_2 \end{bmatrix}, \quad \mathbf{H} = \begin{bmatrix} 0 & 1 \\ -b^2 & -2\xi b \end{bmatrix}, \quad \mathbf{B} = \begin{bmatrix} 0 \\ b^2 \end{bmatrix}.$$

Since $b > 0$ and $\xi > 1$, matrix \mathbf{H} has two distinct real eigenvalues $(-\gamma_1, -\gamma_2)$ with $\gamma_1 > \gamma_2 > 0$ given by

$$\gamma_1 = b(\xi + \sqrt{\xi^2 - 1}), \quad \gamma_2 = b(\xi - \sqrt{\xi^2 - 1}).$$

Standard eigen-decomposition yields

$$\mathbf{H} = \frac{1}{\gamma_1 - \gamma_2} \begin{bmatrix} 1 & 1 \\ -\gamma_2 & -\gamma_1 \end{bmatrix} \begin{bmatrix} -\gamma_2 & 0 \\ 0 & -\gamma_1 \end{bmatrix} \begin{bmatrix} \gamma_1 & 1 \\ -\gamma_2 & -1 \end{bmatrix},$$

and therefore

$$e^{\mathbf{H}t} = \frac{1}{\gamma_1 - \gamma_2} \begin{bmatrix} 1 & 1 \\ -\gamma_2 & -\gamma_1 \end{bmatrix} \begin{bmatrix} e^{-\gamma_2 t} & 0 \\ 0 & e^{-\gamma_1 t} \end{bmatrix} \begin{bmatrix} \gamma_1 & 1 \\ -\gamma_2 & -1 \end{bmatrix}.$$

Using variation of constants, the full solution is

$$\eta(t) = e^{\mathbf{H}t} \eta(0) + \int_0^t e^{\mathbf{H}(t-\tau)} \mathbf{B}u(\tau) d\tau.$$

Evaluating the first component of η gives

$$\eta_1(t) = \eta_{1,h}(t) + \frac{b^2}{\gamma_1 - \gamma_2} \int_0^t (e^{-\gamma_2(t-\tau)} - e^{-\gamma_1(t-\tau)}) u(\tau) d\tau, \quad (58)$$

where $\eta_{1,h}(t)$ is

$$\eta_{1,h}(t) = c_1 e^{-\gamma_1 t} + c_2 e^{-\gamma_2 t}, \quad (59)$$

with

$$c_1 = \frac{-\gamma_2 \eta_{10} - \eta_{20}}{\gamma_1 - \gamma_2}, \quad c_2 = \frac{\gamma_1 \eta_{10} + \eta_{20}}{\gamma_1 - \gamma_2}. \quad (60)$$

Since u is bounded with $\|u\|_\infty = M$, we estimate

$$\begin{aligned} |\eta_1(t)| &\leq |\eta_{1,h}(t)| + \frac{b^2 M}{\gamma_1 - \gamma_2} \int_0^t |e^{-\gamma_2(t-\tau)} - e^{-\gamma_1(t-\tau)}| d\tau \\ &= |\eta_{1,h}(t)| + \frac{b^2 M}{\gamma_1 - \gamma_2} \int_0^t (e^{-\gamma_2(t-\tau)} - e^{-\gamma_1(t-\tau)}) d\tau \\ &= |\eta_{1,h}(t)| + \frac{b^2 M}{\gamma_1 - \gamma_2} \left(\frac{1}{\gamma_2} - \frac{1}{\gamma_1} - \frac{1}{\gamma_2} e^{-\gamma_2 t} + \frac{1}{\gamma_1} e^{-\gamma_1 t} \right). \end{aligned}$$

Noting that $e^{-\gamma_2 t}/\gamma_2 > e^{-\gamma_1 t}/\gamma_1$ for all $t \geq 0$ due to $\gamma_1 > \gamma_2 > 0$ gives

$$\begin{aligned} |\eta_1(t)| &\leq |\eta_{1,h}(t)| + \frac{b^2 M}{\gamma_1 - \gamma_2} \left(\frac{1}{\gamma_2} - \frac{1}{\gamma_1} \right) \\ &= |\eta_{1,h}(t)| + \frac{b^2 M}{\gamma_2 \gamma_1} = |\eta_{1,h}(t)| + M, \end{aligned} \quad (61)$$

since $\gamma_2\gamma_1 = b^2$. Using (59) and (60),

$$|\eta_{1,h}(t)| \leq |c_1|e^{-\gamma_1 t} + |c_2|e^{-\gamma_2 t} \leq |c_1| + |c_2| \leq \frac{\xi|\eta_{10}| + |\eta_{20}|/b}{\sqrt{\xi^2 - 1}}. \quad (62)$$

Combining (61) and (62) gives (56).

Next, we compute $\eta_2(t)$. From (54),(58),(59),

$$\eta_2(t) = \eta_{2,h}(t) + \frac{b^2}{\gamma_1 - \gamma_2} \int_0^t (\gamma_1 e^{-\gamma_1(t-\tau)} - \gamma_2 e^{-\gamma_2(t-\tau)}) u(\tau) d\tau,$$

where $\eta_{2,h}(t)$ is

$$\eta_{2,h}(t) = -\gamma_1 c_1 e^{-\gamma_1 t} - \gamma_2 c_2 e^{-\gamma_2 t}. \quad (63)$$

Using $\|u\|_\infty = M$ gives

$$\begin{aligned} |\eta_2(t)| &\leq |\eta_{2,h}(t)| + \frac{b^2 M}{\gamma_1 - \gamma_2} \int_0^t (\gamma_2 e^{-\gamma_2(t-\tau)} + \gamma_1 e^{-\gamma_1(t-\tau)}) d\tau \\ &= |\eta_{2,h}(t)| + \frac{b^2 M}{\gamma_1 - \gamma_2} (2 - e^{-\gamma_2 t} - e^{-\gamma_1 t}) \\ &\leq |\eta_{2,h}(t)| + \frac{2b^2 M}{\gamma_1 - \gamma_2} = |\eta_{2,h}(t)| + \frac{bM}{\sqrt{\xi^2 - 1}}. \end{aligned} \quad (64)$$

Using (63) and (60),

$$\begin{aligned} |\eta_{2,h}(t)| &\leq \gamma_1 |c_1| e^{-\gamma_1 t} + \gamma_2 |c_2| e^{-\gamma_2 t} \\ &\leq \gamma_1 |c_1| + \gamma_2 |c_2| \leq \frac{b|\eta_{10}| + \xi|\eta_{20}|}{\sqrt{\xi^2 - 1}}. \end{aligned} \quad (65)$$

Combining (64) and (65) gives (57). This completes the proof. \square

Lemma 2 (Karafyllis Lemma on a Shifted Interval). *Let $T_1, T_2 \in \mathbb{R}$ with $0 \leq T_1 < T_2 \leq +\infty$ be given. Consider two absolutely continuous functions $z, V : [T_1, T_2] \rightarrow \mathbb{R}$ for which the following differential inequalities hold for $t \in [T_1, T_2]$ a.e.:*

$$0 \leq \dot{z}(t) \leq \Gamma e^{-z(t)} \max\{W(t) - \varepsilon, 0\}, \quad (66)$$

$$\dot{W}(t) \leq -cW(t) + \frac{\mu}{1 + e^{z(t)}}, \quad (67)$$

for certain constants $c, \varepsilon, \Gamma > 0$ and $\mu \geq 0$. Then the following estimate holds for all $t \in [T_1, T_2]$:

$$\begin{aligned} z(T_1) \leq z(t) \leq \ln \left(\max \left(\frac{\mu}{c\varepsilon} - 1, e^{z(T_1)} \right) \right. \\ \left. + \frac{\Gamma}{c} \max \left\{ W(T_1) + \frac{\mu}{c(1 + e^{z(T_1)})} - \varepsilon, 0 \right\} \right). \end{aligned} \quad (68)$$

The proof follows similar arguments to those of Lemma 4.1 in [38].

B. Proof of Theorem 1

The right-hand side of the closed-loop dynamics (1)-(25) is locally Lipschitz in (\mathbf{x}, z_d, z_q) . Further, from Assumption 2, the grid voltage components satisfy $v_{g,d}, v_{g,q} \in L^\infty(\mathbb{R}_+; \mathbb{R})$. Hence, for every initial condition $(\mathbf{x}(0), z_d(0), z_q(0)) \in \mathbb{R}^{10} \times \mathbb{R} \times \mathbb{R}$ there exists a unique absolutely continuous maximal solution on some interval $[0, t_{\max})$, where $t_{\max} \in (0, +\infty]$.

Boundedness of the filtered reactive powers:

We bound q_1 and q_2 using the second-order filter (10) with input $\text{sat}_{\bar{Q}}(q)$ bounded by \bar{Q} . By Lemma 1 with $b = \omega_{qc}$ and $\xi = \xi_q > 1$,

$$|q_1(t)| \leq \bar{q}_1(\mathbf{x}(0)) := \frac{\xi_q |q_1(0)| + \frac{|q_2(0)|}{\omega_{qc}}}{\sqrt{\xi_q^2 - 1}} + \bar{Q}, \quad (69)$$

$$|q_2(t)| \leq \bar{q}_2(\mathbf{x}(0)) := \frac{\omega_{qc} |q_1(0)| + \xi_q |q_2(0)|}{\sqrt{\xi_q^2 - 1}} + \frac{\omega_{qc} \bar{Q}}{\sqrt{\xi_q^2 - 1}}, \quad (70)$$

for all $t \in [0, t_{\max})$.

d/q-channel error dynamics and storage function bound:

Define the d-axis errors

$$e_{v,d} := v_{c,d} - v_{c,d}^r, \quad e_{i,d} := i_{t,d} - i_{t,d}^r. \quad (71)$$

Using the plant equations, (10),(13), the reference current $i_{t,d}^r$ (17), and (71), we obtain

$$\begin{aligned} \dot{e}_{v,d} &= \omega_b \omega v_{c,q} + \frac{\omega_b}{C_f} (i_{t,d} - i_{g,d}) + K_Q q_2 \\ &= \omega_b \omega v_{c,q} + \frac{\omega_b}{C_f} (e_{i,d} + i_{g,d} - C_f \omega v_{c,q} - \frac{C_f K_Q}{\omega_b} q_2 \\ &\quad - \frac{C_f K_{VC}}{\omega_b} (v_{c,d} - v_{c,d}^r) - i_{g,d}) + K_Q q_2 \\ &= \frac{\omega_b}{C_f} e_{i,d} - K_{VC} e_{v,d}. \end{aligned} \quad (72)$$

Differentiating $e_{i,d}$ and using the plant equations, (10)-(14), and (72),

$$\begin{aligned} \dot{e}_{i,d} &= 2\omega_b \omega (i_{t,q} - i_{g,q}) - \frac{\omega_b R_f}{L_f} i_{t,d} - \omega_b \left(\frac{1}{L_f} + \omega^2 C_f \right) v_{c,d} \\ &\quad - C_f K_P p_2 v_{c,q} + K_{VC} (i_{t,d} - i_{t,d}^r) - \frac{C_f K_{VC}^2}{\omega_b} (v_{c,d} - v_{c,d}^r) \\ &\quad - \frac{C_f K_Q}{\omega_b} \left(2\xi_q \omega_{qc} q_2 + \omega_{qc}^2 (q_1 - \text{sat}_{\bar{Q}}(q)) \right) + \frac{\omega_b}{L_f} v_{t,d} \\ &\quad + \frac{\omega_b R}{L} i_{g,d} - \frac{\omega_b}{L} v_{c,d} + \frac{\omega_b}{L} v_{g,d}. \end{aligned}$$

Choose $v_{t,d}$ as (16), from which it follows

$$\dot{e}_{i,d} = u_d + \frac{\omega_b R}{L} i_{g,d} - \frac{\omega_b}{L} v_{c,d} + \frac{\omega_b}{L} v_{g,d}. \quad (73)$$

Consider the storage function

$$W_d = \frac{1}{2} e_{v,d}^2 + \frac{1}{2} e_{i,d}^2. \quad (74)$$

Using (72) and (73),

$$\begin{aligned} \dot{W}_d &= e_{v,d} \dot{e}_{v,d} + e_{i,d} \dot{e}_{i,d} \\ &= -K_{VC} e_{v,d}^2 + \frac{\omega_b}{C_f} e_{v,d} e_{i,d} + e_{i,d} u_d + \frac{\omega_b R}{L} e_{i,d} i_{g,d} \\ &\quad - \frac{\omega_b}{L} e_{i,d} v_{c,d} + \frac{\omega_b}{L} e_{i,d} v_{g,d}. \end{aligned} \quad (75)$$

Apply Young's inequality with any $\mu_d > 0$ and any $z_d \in \mathbb{R}$:

$$\begin{aligned} \frac{\omega_b R}{L} e_{i,d} i_{g,d} &\leq \frac{(1+e^{z_d})\omega_b^2}{4\mu_d} e_{i,d}^2 i_{g,d}^2 + \frac{\mu_d R^2}{L^2(1+e^{z_d})}, \\ -\frac{\omega_b}{L} e_{i,d} v_{c,d} &\leq \frac{(1+e^{z_d})\omega_b^2}{4\mu_d} e_{i,d}^2 v_{c,d}^2 + \frac{\mu_d}{L^2(1+e^{z_d})}, \\ \frac{\omega_b}{L} e_{i,d} v_{g,d} &\leq \frac{(1+e^{z_d})\omega_b^2}{4\mu_d} e_{i,d}^2 + \frac{\mu_d v_{g,d}^2}{L^2(1+e^{z_d})}. \end{aligned}$$

Thus

$$\begin{aligned} \dot{W}_d &\leq -K_{VC} e_{v,d}^2 + \frac{\omega_b}{C_f} e_{v,d} e_{i,d} + e_{i,d} u_d \\ &+ \frac{(1+e^{z_d})\omega_b^2}{4\mu_d} e_{i,d}^2 (1+i_{g,d}^2+v_{c,d}^2) + \frac{\mu_d(1+R^2+v_{g,d}^2)}{L^2(1+e^{z_d})}. \end{aligned} \quad (76)$$

Choose u_d as prescribed in (18), which cancels the mixed term and dominates the gain-multiplied $e_{i,d}^2$ part in (76). Therefore,

$$\begin{aligned} \dot{W}_d &\leq -K_{VC} e_{v,d}^2 - K_{CC} e_{i,d}^2 + \frac{\mu_d(1+R^2+v_{g,d}^2)}{L^2(1+e^{z_d})} \\ &\leq -2kW_d + \frac{\mu_d(1+R^2+v_{g,d}^2)}{L^2(1+e^{z_d})}, \end{aligned} \quad (77)$$

where $k = \min\{K_{VC}, K_{CC}\}$. The adaptation dynamics satisfy (19), hence $z_d(t)$ is non-decreasing $\implies z_d(t) \geq z_d(0)$ for all $t \in [0, t_{\max})$. Using (77) and $v_{g,d} \in L^\infty$ from Assumption 2,

$$\begin{aligned} W_d(t) &\leq e^{-2kt} W_d(0) + \frac{\mu_d}{L^2} \int_0^t e^{-2k(t-\tau)} \frac{1+R^2+v_{g,d}^2(\tau)}{1+e^{z_d(\tau)}} d\tau \\ &\leq e^{-2kt} W_d(0) + \frac{\mu_d(1+R^2+\|v_{g,d}\|_\infty^2)}{2kL^2(1+e^{z_d(0)})} (1-e^{-2kt}) \\ &\leq e^{-2kt} W_d(0) + \frac{\mu_d(1+R^2+\|v_{g,d}\|_\infty^2)}{2kL^2(1+e^{z_d(0)})}. \end{aligned} \quad (78)$$

Since $e_{v,d}^2, e_{i,d}^2 \leq 2W_d$, we get for all $t \in [0, t_{\max})$

$$|e_{v,d}(t)|, |e_{i,d}(t)| \leq \sqrt{2W_d(0) + \frac{\mu_d(1+R^2+\|v_{g,d}\|_\infty^2)}{kL^2(1+e^{z_d(0)})}}. \quad (79)$$

Similarly, for the q- channel, for error variables defined as

$$e_{v,q} := v_{c,q} - v_{c,q}^r, \quad e_{i,q} := i_{t,q} - i_{t,q}^r,$$

it holds that

$$|e_{v,q}(t)|, |e_{i,q}(t)| \leq \sqrt{2W_q(0) + \frac{\mu_q(1+R^2+\|v_{g,q}\|_\infty^2)}{kL^2(1+e^{z_q(0)})}},$$

$t \in [0, t_{\max})$.

Boundedness of the PCC voltage:

From the reactive power-voltage droop (13) and using (69), we have for $t \in [0, t_{\max})$,

$$|v_{c,d}^r(t)| \leq |V_0 + K_Q Q_0| + |K_Q| \bar{q}_1.$$

Further, noting that $v_{c,d} = v_{c,d}^r + e_{v,d}$ and $|v_{c,d}| \leq |v_{c,d}^r| + |e_{v,d}|$, and combining with the error bound (79), we obtain

$$\begin{aligned} |v_{c,d}(t)| &\leq \bar{v}_{c,d}(\mathbf{x}(0), z_d(0), \|v_{g,d}\|_\infty) \\ &:= \sqrt{2W_d(0) + \frac{\mu_d(1+R^2+\|v_{g,d}\|_\infty^2)}{kL^2(1+e^{z_d(0)})}} \\ &\quad + |V_0 + K_Q Q_0| + |K_Q| \bar{q}_1, \end{aligned} \quad (80)$$

for all $t \in [0, t_{\max})$. Repeating similar steps, we obtain

$$\begin{aligned} |v_{c,q}(t)| &\leq \bar{v}_{c,q}(\mathbf{x}(0), z_q(0), \|v_{g,q}\|_\infty) \\ &:= \sqrt{2W_q(0) + \frac{\mu_q(1+R^2+\|v_{g,q}\|_\infty^2)}{kL^2(1+e^{z_q(0)})}}, \end{aligned} \quad (81)$$

for all $t \in [0, t_{\max})$.

Boundedness of the grid current:

Let

$$W_1 := \frac{1}{2}(i_{g,d}^2 + i_{g,q}^2).$$

From the grid-inductor dynamics (5) and (6),

$$\begin{aligned} \dot{W}_1 &= -\frac{\omega_b R}{L} (i_{g,d}^2 + i_{g,q}^2) + \frac{\omega_b}{L} i_{g,d} (v_{c,d} - v_{g,d}) \\ &\quad + \frac{\omega_b}{L} i_{g,q} (v_{c,q} - v_{g,q}). \end{aligned} \quad (82)$$

Applying Young's inequality repeatedly gives

$$\begin{aligned} \frac{\omega_b}{L} i_{g,d} (v_{c,d} - v_{g,d}) &\leq \frac{\omega_b^2}{2L^2} \delta_1 i_{g,d}^2 + \frac{1}{2\delta_1} (v_{c,d} - v_{g,d})^2 \\ &\leq \frac{\omega_b^2}{2L^2} \delta_1 i_{g,d}^2 + \frac{1}{\delta_1} (v_{c,d}^2 + v_{g,d}^2), \end{aligned} \quad (83)$$

and

$$\begin{aligned} \frac{\omega_b}{L} i_{g,q} (v_{c,q} - v_{g,q}) &\leq \frac{\omega_b^2}{2L^2} \delta_1 i_{g,q}^2 + \frac{1}{2\delta_1} (v_{c,q} - v_{g,q})^2 \\ &\leq \frac{\omega_b^2}{2L^2} \delta_1 i_{g,q}^2 + \frac{1}{\delta_1} (v_{c,q}^2 + v_{g,q}^2), \end{aligned} \quad (84)$$

for some $\delta_1 > 0$. Choosing $\delta_1 = \frac{LR}{\omega_b}$, substituting (83) and (84) in (82), and since $i_{g,d}^2 + i_{g,q}^2 = 2W_1$ and $v_{g,d}, v_{g,q} \in L^\infty$,

$$\begin{aligned} \dot{W}_1 &\leq -\frac{\omega_b R}{L} W_1 + \frac{\omega_b}{LR} (v_{c,d}^2 + v_{c,q}^2 + v_{g,d}^2 + v_{g,q}^2) \\ &\leq -\frac{\omega_b R}{L} W_1 + \frac{\omega_b}{LR} (\bar{v}_{c,d}^2 + \bar{v}_{c,q}^2 + \|v_{g,d}\|_\infty^2 + \|v_{g,q}\|_\infty^2), \end{aligned}$$

where $\bar{v}_{c,d}, \bar{v}_{c,q} > 0$ are the bounds on $|v_{c,d}|, |v_{c,q}|$ given in (80) and (81). From this, it follows

$$W_1(t) \leq e^{-\frac{\omega_b R}{L} t} W_1(0) + \frac{\bar{v}_{c,d}^2 + \bar{v}_{c,q}^2 + \|v_{g,d}\|_\infty^2 + \|v_{g,q}\|_\infty^2}{R^2},$$

for all $t \in [0, t_{\max})$. Hence, noting that $i_{g,d}^2, i_{g,q}^2 \leq 2W_1$, we obtain

$$\begin{aligned} |i_{g,d}(t)|, |i_{g,q}(t)| &\leq \bar{i}_g(\mathbf{x}(0), z_d(0), z_q(0), \|v_{g,d}\|_\infty, \|v_{g,q}\|_\infty) \\ &:= \sqrt{i_{g,d}^2(0) + i_{g,q}^2(0) + \frac{2(\bar{v}_{c,d}^2 + \bar{v}_{c,q}^2 + \|v_{g,d}\|_\infty^2 + \|v_{g,q}\|_\infty^2)}{R^2}}, \end{aligned} \quad (85)$$

for all $t \in [0, t_{\max})$.

Boundedness of the filtered active powers:

We bound p_1 and p_2 using the second-order filter (11). From (8) and the bounds (80),(81),(85), it holds that $|p| \leq \bar{i}_g(\bar{v}_{c,d} +$

$\bar{v}_{c,q}$) for all $t \in [0, t_{\max}]$. Since $|\text{sat}_{\bar{P}}(y)| \leq |y|$ for all $y \in \mathbb{R}$ and all $\bar{P} \in (0, +\infty)$, we get $|\text{sat}_{\bar{P}}(p(t))| \leq \bar{i}_g(\bar{v}_{c,d} + \bar{v}_{c,q}), \forall t \in [0, t_{\max}]$. Then, by Lemma 1 with $b = \omega_{pc}$ and $\xi = \xi_p > 1$,

$$\begin{aligned} |p_1(t)| &\leq \bar{p}_1(\mathbf{x}(0), z_d(0), z_q(0), \|v_{g,d}\|_\infty, \|v_{g,q}\|_\infty) \\ &:= \frac{\xi_p |p_1(0)| + \frac{|p_2(0)|}{\omega_{pc}}}{\sqrt{\xi_p^2 - 1}} + \bar{i}_g(\bar{v}_{c,d} + \bar{v}_{c,q}), \end{aligned} \quad (86)$$

$$\begin{aligned} |p_2(t)| &\leq \bar{p}_2(\mathbf{x}(0), z_d(0), z_q(0), \|v_{g,d}\|_\infty, \|v_{g,q}\|_\infty) \\ &:= \frac{\omega_{pc}|p_1(0)| + \xi_p |p_2(0)|}{\sqrt{\xi_p^2 - 1}} + \frac{\omega_{pc}(\bar{i}_g(\bar{v}_{c,d} + \bar{v}_{c,q}))}{\sqrt{\xi_p^2 - 1}}, \end{aligned} \quad (87)$$

for all $t \in [0, t_{\max}]$.

Boundedness of the terminal current:

Next, for $i_{t,d}$, observe from (17) that

$$|i_{t,d}^r| \leq |i_{g,d}| + C_f |\omega| |v_{c,q}| + \frac{C_f |K_Q|}{\omega_b} |q_2| + \frac{C_f K_{VC}}{\omega_b} |e_{v,d}|.$$

The active power-frequency droop (14) and (86) imply

$$|\omega| \leq |\omega_0 + K_P P_0| + |K_P \bar{p}_1|.$$

Therefore, using (70),(81),(85),

$$\begin{aligned} |i_{t,d}^r| &\leq \bar{i}_g + C_f (|\omega_0 + K_P P_0| + |K_P \bar{p}_1|) \bar{v}_{c,q} + \frac{C_f |K_Q|}{\omega_b} \bar{q}_2 \\ &\quad + \frac{C_f K_{VC}}{\omega_b} |e_{v,d}|. \end{aligned}$$

Finally, $i_{t,d} = i_{t,d}^r + e_{i,d}$ together with the bound (79) on $e_{i,d}$ and $e_{v,d}$ gives

$$\begin{aligned} |i_{t,d}| &\leq \bar{i}_g + C_f (|\omega_0 + K_P P_0| + |K_P \bar{p}_1|) \bar{v}_{c,q} + \frac{C_f |K_Q|}{\omega_b} \bar{q}_2 \\ &\quad + \left(\frac{C_f K_{VC}}{\omega_b} + 1 \right) \sqrt{2W_d(0) + \frac{\mu_d(1 + R^2 + \|v_{g,d}\|_\infty^2)}{kL^2(1 + e^{z_d(0)})}}, \end{aligned}$$

$t \in [0, t_{\max}]$. Similar derivation on the q-axis yields

$$\begin{aligned} |i_{t,q}(t)| &\leq \bar{i}_g + C_f (|\omega_0 + K_P P_0| + |K_P \bar{p}_1|) \bar{v}_{c,d} \\ &\quad + \left(\frac{C_f K_{VC}}{\omega_b} + 1 \right) \sqrt{2W_q(0) + \frac{\mu_q(1 + R^2 + \|v_{g,q}\|_\infty^2)}{kL^2(1 + e^{z_q(0)})}}, \end{aligned}$$

$t \in [0, t_{\max}]$.

Boundedness of the adaptive gains:

Considering (19),(20),(77), recalling that $|v_{g,d}(t)| \leq \|v_{g,d}\|_\infty$ a.e, applying Lemma 2, and noting that z_d is non-decreasing, we obtain

$$\begin{aligned} z_d(0) &\leq z_d(t) \leq \ln \left(\max \left\{ \frac{\mu_d(1 + R^2 + \|v_{g,d}\|_\infty^2)}{2kL^2\varepsilon} - 1, e^{z_d(0)} \right\} \right. \\ &\quad \left. + \frac{\Gamma_d}{2k} \max \left\{ W_d(0) + \frac{\mu_d(1 + R^2 + \|v_{g,d}\|_\infty^2)}{2kL^2(1 + e^{z_d(0)})} - \varepsilon, 0 \right\} \right), \end{aligned} \quad (88)$$

for all $t \in [0, t_{\max}]$. Similarly, we can obtain the upper bound for z_q .

Since all the states $(\mathbf{x}(t), z_d(t), z_q(t))$ are bounded, $t_{\max} = +\infty$. Therefore, the unique absolutely continuous solution exists for all $t \geq 0$, and the bounds derived above hold for all $t \geq 0$. This completes the proof. \square

C. Proof of Theorem 2

Consider the d-channel storage function W_d in (74). Since $(v_{c,d} - v_{c,d}^r)^2 \leq 2W_d$ for all $t \geq 0$ and $1 + e^{z_d(0)} > 1$, the estimate (34) directly follows from (78).

The estimate (88) together with the fact that z_d is non-decreasing (note from (19) that $\dot{z}_d(t) \geq 0$ a.e.), implies that z_d has a finite limit as $t \rightarrow +\infty$. As a result, e^{z_d} also has a finite limit as $t \rightarrow +\infty$. Recall that \dot{W}_d is given by (75). There, $v_{g,d} \in L^\infty(\mathbb{R}_+; \mathbb{R})$; the terms $e_{v,d}, e_{i,d}$ are bounded due to (79); the signals $i_{g,d}$ and $v_{c,d}$ are bounded by Theorem 1; and u_d in (18) is bounded because all states are bounded by Theorem 1. Therefore, \dot{W}_d is bounded. As a result,

$$\frac{d}{dt} e^{z_d} = \Gamma_d \max\{W_d - \varepsilon, 0\},$$

is uniformly continuous. Furthermore, we have

$$\int_0^{+\infty} \frac{d}{dt} e^{z_d} dt = \lim_{t \rightarrow +\infty} (e^{z_d} - e^{z_d(0)}) < +\infty.$$

Then, from Barbalat's Lemma

$$\lim_{t \rightarrow +\infty} \left(\frac{d}{dt} e^{z_d} \right) = \Gamma_d \lim_{t \rightarrow +\infty} (\max\{W_d - \varepsilon, 0\}) = 0.$$

Therefore,

$$\limsup_{t \rightarrow +\infty} W_d \leq \varepsilon,$$

and hence $\limsup_{t \rightarrow +\infty} |e_{v,d}(t)| \leq \sqrt{2\varepsilon}$.

A verbatim repetition of the above steps for the q-channel yields (35) and (38). This completes the proof. \square

D. Proof of Theorem 4

The right-hand side of the closed-loop dynamics (1)–(15) with the control input $\mathbf{v}_t = [v_{t,d}, v_{t,q}]^\top$ given by (45),(44), where the nominal input $\mathbf{v}_t^n = [v_{t,d}^n, v_{t,q}^n]^\top$ is any locally Lipschitz controller $\mathbf{k}(\mathbf{x})$ with $\mathbf{k} : \mathbb{R}^{10} \rightarrow \mathbb{R}^2$, is itself locally Lipschitz in the state. This is because, the safety filtered control (44),(45) is obtained by projecting \mathbf{v}_t^n onto a closed half-space defined by the affine CBF constraint, which yields a locally Lipschitz mapping in \mathbf{x} on the set $\{\|\dot{\mathbf{i}}_t\| \neq 0\}$. Moreover, when $\|\dot{\mathbf{i}}_t\| = 0$, all terms in (44) that depend on $\dot{\mathbf{i}}_t$ vanish and $h(\mathbf{x}) = I_{\max}^2$, so that $\eta(\mathbf{x}, \mathbf{v}_t^n) = cI_{\max}^2 > 0$. By continuity of $\eta(\mathbf{x}, \mathbf{v}_t^n)$, there exists $\epsilon > 0$ such that $\eta(\mathbf{x}, \mathbf{v}_t^n) \geq 0$ for all \mathbf{x} satisfying $\|\dot{\mathbf{i}}_t\| < \epsilon$. Hence, in a neighborhood of the set $\{\|\dot{\mathbf{i}}_t\| = 0\}$ the safety filter is inactive and $\mathbf{v}_t = \mathbf{v}_t^n$, which implies that \mathbf{v}_t is locally Lipschitz in that neighborhood. Thus, the closed-loop vector field is locally Lipschitz in \mathbf{x} . Further, from Assumption 2, the grid voltage components satisfy $v_{g,d}, v_{g,q} \in L^\infty(\mathbb{R}_+; \mathbb{R})$. Thus, for every initial condition $\mathbf{x}(0) \in \mathbb{R}^{10}$, there exists a unique absolutely continuous maximal solution $\mathbf{x}(t)$ defined on some interval $[0, t_{\max})$, where $t_{\max} \in (0, +\infty]$.

Terminal current safety:

With the barrier function $h(\mathbf{x}) = I_{\max}^2 - \|\mathbf{i}_t\|^2$, the constraint in the QP (43) enforces $\dot{h}(\mathbf{x}(t)) \geq -ch(\mathbf{x}(t))$ a.e for all $t \in [0, t_{\max}]$. Thus, for all $t \in [0, t_{\max}]$,

$$h(t) \geq e^{-ct}h(0) \Rightarrow h(t) \geq 0 \text{ whenever } h(0) \geq 0.$$

Equivalently, $\|\mathbf{i}_t(t)\| \leq I_{\max}$ for all $t \in [0, t_{\max}]$.

Boundedness of the PCC voltage and grid current:

Let $\mathbf{v}_c = [v_{c,d}, v_{c,q}]^\top$, $\mathbf{v}_g = [v_{g,d}, v_{g,q}]^\top$, and $\mathbf{i}_g = [i_{g,d}, i_{g,q}]^\top$. Concatenating the corresponding dynamics (1),(2) and (5),(6), we obtain

$$\dot{\mathbf{v}}_c = \omega_b \omega \mathbf{J} \mathbf{v}_c + \frac{\omega_b}{C_f} (\mathbf{i}_t - \mathbf{i}_g), \quad (89)$$

$$\dot{\mathbf{i}}_g = \omega_b \omega \mathbf{J} \mathbf{i}_g + \frac{\omega_b}{L} (\mathbf{v}_c - \mathbf{v}_g) - \frac{\omega_b R}{L} \dot{\mathbf{i}}_g, \quad (90)$$

where

$$\mathbf{J} = \begin{bmatrix} 0 & 1 \\ -1 & 0 \end{bmatrix}. \quad (91)$$

Consider the storage function

$$W_2 = \frac{1}{2} C_f \|\mathbf{v}_c\|^2 + \frac{1}{2} L \|\mathbf{i}_g\|^2 + \lambda \mathbf{v}_c^\top \mathbf{i}_g, \quad 0 < |\lambda| < \sqrt{C_f L}.$$

with λ to be chosen later. Completing the square gives

$$W_2 = \frac{1}{2} C_f \left\| \mathbf{v}_c + \frac{\lambda}{C_f} \mathbf{i}_g \right\|^2 + \frac{1}{2} \left(L - \frac{\lambda^2}{C_f} \right) \|\mathbf{i}_g\|^2,$$

which is positive definite provided $|\lambda| < \sqrt{C_f L}$. Using (89)-(91), we obtain

$$\begin{aligned} \dot{W}_2 &= C_f \mathbf{v}_c^\top \dot{\mathbf{v}}_c + L \dot{\mathbf{i}}_g^\top \mathbf{i}_g + \lambda \mathbf{v}_c^\top \dot{\mathbf{i}}_g + \lambda \dot{\mathbf{i}}_g^\top \mathbf{v}_c \\ &= C_f \mathbf{v}_c^\top \left(\omega_b \omega \mathbf{J} \mathbf{v}_c + \frac{\omega_b}{C_f} (\mathbf{i}_t - \mathbf{i}_g) \right) \\ &\quad + L \dot{\mathbf{i}}_g^\top \left(\omega_b \omega \mathbf{J} \mathbf{i}_g + \frac{\omega_b}{L} (\mathbf{v}_c - \mathbf{v}_g) - \frac{\omega_b R}{L} \dot{\mathbf{i}}_g \right) \\ &\quad + \lambda \mathbf{v}_c^\top \left(\omega_b \omega \mathbf{J} \mathbf{i}_g + \frac{\omega_b}{L} (\mathbf{v}_c - \mathbf{v}_g) - \frac{\omega_b R}{L} \dot{\mathbf{i}}_g \right) \\ &\quad + \lambda \dot{\mathbf{i}}_g^\top \left(\omega_b \omega \mathbf{J} \mathbf{v}_c + \frac{\omega_b}{C_f} (\mathbf{i}_t - \mathbf{i}_g) \right), \end{aligned}$$

and, using the skew-symmetry of \mathbf{J} , we get

$$\begin{aligned} \dot{W}_2 &= \omega_b \mathbf{v}_c^\top \dot{\mathbf{i}}_t - \omega_b \dot{\mathbf{i}}_g^\top \mathbf{v}_g - \omega_b R \|\dot{\mathbf{i}}_g\|^2 \\ &\quad + \lambda \omega_b \left(\frac{1}{L} \|\mathbf{v}_c\|^2 - \frac{1}{L} \mathbf{v}_c^\top \mathbf{v}_g - \frac{R}{L} \mathbf{v}_c^\top \mathbf{i}_g + \frac{1}{C_f} \dot{\mathbf{i}}_g^\top \mathbf{i}_t \right. \\ &\quad \left. - \frac{1}{C_f} \|\mathbf{i}_g\|^2 \right). \end{aligned}$$

Applying Young's inequalities with constants $\delta_2, \delta_3, \delta_4 > 0$,

$$\begin{aligned} \omega_b \mathbf{v}_c^\top \dot{\mathbf{i}}_t &\leq \omega_b \left(\frac{\delta_2}{2} \|\mathbf{v}_c\|^2 + \frac{1}{2\delta_2} \|\dot{\mathbf{i}}_t\|^2 \right), \\ -\omega_b \dot{\mathbf{i}}_g^\top \mathbf{v}_g &\leq \omega_b \left(\frac{R}{2} \|\mathbf{i}_g\|^2 + \frac{1}{2R} \|\mathbf{v}_g\|^2 \right), \\ -\lambda \omega_b \frac{1}{L} \mathbf{v}_c^\top \mathbf{v}_g &\leq |\lambda| \omega_b \left(\frac{1}{2L} \|\mathbf{v}_c\|^2 + \frac{1}{2L} \|\mathbf{v}_g\|^2 \right), \\ -\lambda \omega_b \frac{R}{L} \mathbf{v}_c^\top \mathbf{i}_g &\leq |\lambda| \omega_b \frac{R}{L} \left(\frac{\delta_3}{2} \|\mathbf{v}_c\|^2 + \frac{1}{2\delta_3} \|\mathbf{i}_g\|^2 \right), \\ \lambda \omega_b \frac{1}{C_f} \dot{\mathbf{i}}_g^\top \mathbf{i}_t &\leq |\lambda| \omega_b \left(\frac{\delta_4}{2C_f} \|\mathbf{i}_g\|^2 + \frac{1}{2\delta_4 C_f} \|\dot{\mathbf{i}}_t\|^2 \right). \end{aligned}$$

Hence,

$$\begin{aligned} \dot{W}_2 &\leq \omega_b \left(\frac{\delta_2}{2} + \frac{\lambda}{L} + \frac{|\lambda|}{2L} + \frac{|\lambda|R\delta_3}{2L} \right) \|\mathbf{v}_c\|^2 \\ &\quad + \omega_b \left(-\frac{R}{2} + \frac{|\lambda|R}{2L\delta_3} + \frac{|\lambda|\delta_4}{2C_f} + \frac{|\lambda|}{C_f} \right) \|\mathbf{i}_g\|^2 \\ &\quad + \omega_b \left(\frac{1}{2\delta_2} + \frac{|\lambda|}{2\delta_4 C_f} \right) \|\dot{\mathbf{i}}_t\|^2 + \omega_b \left(\frac{1}{2R} + \frac{|\lambda|}{2L} \right) \|\mathbf{v}_g\|^2. \end{aligned}$$

Let $\delta_2 = \frac{|\lambda|}{4L}, \delta_3 = \frac{1}{2R}, \delta_4 = 1$, which yields

$$\begin{aligned} \dot{W}_2 &\leq \omega_b \left(\frac{8\lambda + 7|\lambda|}{8L} \right) \|\mathbf{v}_c\|^2 \\ &\quad + \omega_b \left(-\frac{R}{2} + |\lambda| \left(\frac{R^2}{L} + \frac{3}{2C_f} \right) \right) \|\mathbf{i}_g\|^2 \\ &\quad + \omega_b \left(\frac{2L}{|\lambda|} + \frac{|\lambda|}{2C_f} \right) \|\dot{\mathbf{i}}_t\|^2 + \omega_b \left(\frac{1}{2R} + \frac{|\lambda|}{2L} \right) \|\mathbf{v}_g\|^2. \end{aligned}$$

Choose $\lambda < 0$ such that

$$-\min \left\{ \sqrt{C_f L}, \frac{R}{4 \left(\frac{R^2}{L} + \frac{3}{2C_f} \right)} \right\} < \lambda < 0.$$

With this, the $\|\mathbf{v}_c\|^2$ and $\|\mathbf{i}_g\|^2$ coefficients are strictly negative, and we obtain

$$\dot{W}_2 \leq -k_1 (\|\mathbf{v}_c\|^2 + \|\mathbf{i}_g\|^2) + k_2 \|\dot{\mathbf{i}}_t\|^2 + k_3 \|\mathbf{v}_g\|^2,$$

where $k_1 = \min \left\{ \frac{\omega_b |\lambda|}{8L}, \frac{\omega_b R}{4} \right\}$, $k_2 = \omega_b \left(\frac{2L}{|\lambda|} + \frac{|\lambda|}{2C_f} \right)$, and $k_3 = \omega_b \left(\frac{1}{2R} + \frac{|\lambda|}{2L} \right)$. Then, recall that $\|\mathbf{i}_t(t)\| \leq I_{\max}$ for all $t \in [0, t_{\max}]$. By Assumption 2, $\|\mathbf{v}_g\|$ is essentially bounded. Furthermore, since W_2 is positive definite in $(\|\mathbf{v}_c\|, \|\mathbf{i}_g\|)$, there exists $\bar{c} > \underline{c} > 0$ such that

$$\underline{c} (\|\mathbf{v}_c\|^2 + \|\mathbf{i}_g\|^2) \leq W_2 \leq \bar{c} (\|\mathbf{v}_c\|^2 + \|\mathbf{i}_g\|^2). \quad (92)$$

Therefore, noting that $\|\mathbf{v}_g\|_\infty^2 \leq \|v_{g,d}\|_\infty^2 + \|v_{g,q}\|_\infty^2$,

$$\dot{W}_2(t) \leq -k_4 W_2(t) + k_2 I_{\max}^2 + k_3 (\|v_{g,d}\|_\infty^2 + \|v_{g,q}\|_\infty^2),$$

for $t \in [0, t_{\max}]$ a.e., where $k_4 = k_1/\bar{c} > 0$. By comparison,

$$W_2(t) \leq e^{-k_4 t} W_2(0) + \frac{k_2}{k_4} I_{\max}^2 + \frac{k_3}{k_4} (\|v_{g,d}\|_\infty^2 + \|v_{g,q}\|_\infty^2), \quad (93)$$

for all $t \in [0, t_{\max}]$. Again considering (92), we deduce from (93) that there exists a function $\tilde{B}_{2,\Omega} \in C^0(\mathbb{R}^2 \times \mathbb{R}^2 \times \mathbb{R}_+ \times \mathbb{R}_+)$ such that

$$\|[\mathbf{v}_c^\top(t), \dot{\mathbf{i}}_g^\top(t)]^\top\| \leq \tilde{B}_{2,\Omega}(\mathbf{v}_c(0), \mathbf{i}_g(0), \|v_{g,d}\|_\infty, \|v_{g,q}\|_\infty), \quad (94)$$

for all $t \in [0, t_{\max}]$.

Boundedness of the power filters:

The instantaneous powers satisfy $p = \mathbf{v}_c^\top \dot{\mathbf{i}}_g$ and $q = \mathbf{v}_c^\top \mathbf{J}^\top \dot{\mathbf{i}}_g$, so there exists $c_p, c_q > 0$ such that $|p(t)| \leq c_p \|[\mathbf{v}_c^\top(t), \dot{\mathbf{i}}_g^\top(t)]^\top\|^2$ and $|q(t)| \leq c_q \|[\mathbf{v}_c^\top(t), \dot{\mathbf{i}}_g^\top(t)]^\top\|^2$, hence it follows from (94) that $p, q \in L^\infty$. Since $|\text{sat}_{\bar{P}}(p)| \leq |p|$ and $|\text{sat}_{\bar{Q}}(q)| \leq |q|$ for all $p, q \in \mathbb{R}$ and all $\bar{P}, \bar{Q} \in$

$(0, +\infty]$, we get $|\text{sat}_{\overline{p}}(p(t))| \leq \|p\|_\infty$ and $|\text{sat}_{\overline{q}}(q(t))| \leq \|q\|_\infty$ for all $t \in [0, t_{\max})$. Then, using Lemma 1,

$$\begin{aligned} |p_1(t)| &\leq \frac{\xi_p |p_1(0)| + \frac{|p_2(0)|}{\omega_{pc}}}{\sqrt{\xi_p^2 - 1}} + \|p\|_\infty, \\ |q_1(t)| &\leq \frac{\xi_q |q_1(0)| + \frac{|q_2(0)|}{\omega_{qc}}}{\sqrt{\xi_q^2 - 1}} + \|q\|_\infty, \\ |p_2(t)| &\leq \frac{\omega_{pc} |p_1(0)| + \xi_p |p_2(0)|}{\sqrt{\xi_p^2 - 1}} + \frac{\omega_{pc} \|p\|_\infty}{\sqrt{\xi_p^2 - 1}}, \\ |q_2(t)| &\leq \frac{\omega_{qc} |q_1(0)| + \xi_q |q_2(0)|}{\sqrt{\xi_q^2 - 1}} + \frac{\omega_{qc} \|q\|_\infty}{\sqrt{\xi_q^2 - 1}}, \end{aligned}$$

for all $t \in [0, t_{\max})$.

Since all the components of $\mathbf{x}(t)$ are bounded, we have that $t_{\max} = +\infty$. Therefore, the unique absolutely continuous solution exists for all $t \geq 0$, and the bounds derived above hold for all $t \geq 0$. This completes the proof. \square

E. Proof of Proposition 1

Following similar arguments to those in the proof of Theorem 4, it can be shown that for every initial condition $(\mathbf{x}(0), z_d(0), z_q(0)) \in \mathbb{R}^{10} \times \mathbb{R} \times \mathbb{R}$, there exists a unique maximal solution $(\mathbf{x}(t), z_d, z_q)$ defined on some interval $[0, t_{\max})$, where $t_{\max} \in (0, +\infty]$. Furthermore, similar to as shown in the proof of Theorem 4, it can be shown that $i_{t,d}, i_{t,q}$ and \mathbf{x}' satisfy (47),(48) on $[0, t_{\max})$. Therefore, \mathbf{x} is bounded on $[0, t_{\max})$. This implies the boundedness of W_d and W_q on $[0, t_{\max})$ that enter the adaptation laws for z_d and z_q (see (13),(14),(17),(19),(20),(22),(24),(25)). Considering the d channel, since $\max\{W_d - \varepsilon, 0\} \geq 0$, we have $\dot{z}_d(t) \geq 0$ a.e. on $[0, t_{\max})$, so z_d is non-decreasing and $z_d(t) \geq z_d(0)$. Moreover, $\frac{d}{dt} e^{z_d} = e^{z_d} \dot{z}_d(t) = \Gamma_d \max\{W_d - \varepsilon, 0\}$. Since $W_d \in L^\infty([0, t_{\max}); \mathbb{R})$, then $\frac{d}{dt} e^{z_d}$ is essentially bounded on $[0, t_{\max})$, and therefore $e^{z_d(t)}$ (hence $z_d(t)$) cannot blow up in finite time. An analogous argument holds for z_q . Therefore, $t_{\max} = +\infty$ and the closed-loop system has a unique absolutely continuous solution for all $t \geq 0$.

F. Proof of Theorem 5

In the proof of Proposition 1, it is established that the bounds (47),(48) hold on some interval $[0, t_{\max})$, where $t_{\max} \in (0, +\infty]$. Since the unique absolutely continuous solution of the closed-loop system exists for all $t \geq 0$ (see Proposition 1), we conclude that the bounds (47),(48) hold for all $t \geq 0$.

Let us now proceed to establish (53). For brevity, we consider the d- component only. Since \mathbf{x} is bounded as in (47),(48), there exists a continuous function

$$\overline{W}_d = \overline{W}_d(\mathbf{x}(0), \|v_{g,d}\|_\infty, \|v_{g,q}\|_\infty), \quad (95)$$

such that

$$0 \leq W_d(t) \leq \overline{W}_d, \quad (96)$$

for all $t \geq 0$, where W_d is given by (20).

We first estimate the growth of z_d that can be attributed to the ON episodes \mathcal{I}_{on} (50). From (19), $\dot{z}_d(t) \geq 0$ a.e., and hence z_d is non-decreasing. Therefore, using (95) and the fact that $z_d(t) \geq z_d(0)$ for all $t \geq 0$, we obtain from (19), for all $t \in \mathcal{I}_{\text{on}}$ a.e.,

$$\dot{z}_d(t) \leq \Gamma_d e^{-z_d(0)} \max\{\overline{W}_d - \varepsilon, 0\}.$$

Integrating over the ON times gives the bound

$$\begin{aligned} \int_{\mathcal{I}_{\text{on}}} \dot{z}_d(s) ds &\leq \Gamma_d e^{-z_d(0)} \max\{\overline{W}_d - \varepsilon, 0\} \int_{\mathcal{I}_{\text{on}}} 1 ds \\ &\leq \Gamma_d e^{-z_d(0)} \max\{\overline{W}_d - \varepsilon, 0\} T_\Omega =: \Delta z_d^{\text{on}}. \end{aligned} \quad (97)$$

Above, we have used from Assumption 3 that $\int_{\mathcal{I}_{\text{on}}} 1 ds = T_\eta \leq T_\Omega$. Note that Δz_d^{on} depends continuously on $\mathbf{x}(0), z_d(0), \|v_{g,d}\|_\infty, \|v_{g,q}\|_\infty$, and linearly on T_Ω .

Next we focus on the behavior of z_d in OFF episodes. Define the OFF set

$$\mathcal{I}_{\text{off}} := [0, +\infty) \setminus \mathcal{I}_{\text{on}} = \{t \geq 0 : \eta(t) \geq 0\}.$$

Since \mathcal{I}_{on} is a finite union (at most N_Ω) of disjoint intervals of the form $[0, \sigma_0)$ (if $\eta(0) < 0$) and $(\tau_\kappa, \sigma_\kappa)$, $\kappa \in \mathcal{J}$, \mathcal{I}_{off} is a finite union of disjoint closed intervals, with the last one unbounded on the right (see Remark 4). That is, there exist $N_{\text{off}} \in \mathbb{N} \cup \{0\}$ and points

$$0 \leq s_0 \leq t_0 \leq s_1 \leq t_1 \leq \dots \leq s_{N_{\text{off}}-1} \leq t_{N_{\text{off}}-1} \leq s_{N_{\text{off}}} < +\infty,$$

such that

$$\mathcal{I}_{\text{off}} = \bigcup_{\kappa=0}^{N_{\text{off}}-1} [s_\kappa, t_\kappa] \cup [s_{N_{\text{off}}}, +\infty),$$

where each $[s_\kappa, t_\kappa]$ is a closed interval ($s_\kappa = t_\kappa$ is allowed). Moreover, since \mathcal{I}_{on} has N_η intervals, \mathcal{I}_{off} has at most $N_\eta + 1$ intervals, and thus

$$N_{\text{off}} \leq N_\eta \leq N_\Omega. \quad (98)$$

On each OFF interval $J_\kappa = [s_\kappa, t_\kappa] \subseteq \mathcal{I}_{\text{off}}$, where $\kappa = 0, \dots, N_{\text{off}} - 1$, the controller coincides with the DADS-BN nominal controller. Therefore, similar to that in the proof of Theorem 1, we can show

$$\dot{W}_d(t) \leq -2kW_d(t) + \frac{\mu_d^{\text{eff}}}{1 + e^{z_d(t)}},$$

on J_κ a.e., where

$$\mu_d^{\text{eff}} := \frac{\mu_d(1 + R^2 + \|v_{g,d}\|_\infty^2)}{L^2},$$

and k is given by (36). Together with (19), this matches the hypotheses of Lemma 2 on $[T_1, T_2) = [s_\kappa, t_\kappa)$. If $t_\kappa > s_\kappa$, Lemma 2 yields, for all $t \in J_\kappa$,

$$\begin{aligned} z_d(s_\kappa) &\leq z_d(t) \\ &\leq \ln \left(\max \left(\frac{\mu_d^{\text{eff}}}{2k\varepsilon} - 1, e^{z_d(s_\kappa)} \right) \right. \\ &\quad \left. + \frac{\Gamma_d}{2k} \max \left\{ W_d(s_\kappa) + \frac{\mu_d^{\text{eff}}}{2k(1 + e^{z_d(s_\kappa)})} - \varepsilon, 0 \right\} \right). \end{aligned} \quad (99)$$

If $t_\kappa = s_\kappa$, then J_κ reduces to a single point and $z_d(t_\kappa) = z_d(s_\kappa)$, so (99) holds trivially.

With (97) and (99) at hand, below we work on obtaining an ultimate bound on $z_d(t)$. Define the continuous function $\Phi_d : \mathbb{R} \rightarrow \mathbb{R}$ by

$$\Phi_d(\zeta) := \ln \left(\max \left(\frac{\mu_d^{\text{eff}}}{2k\varepsilon} - 1, e^\zeta \right) + \frac{\Gamma_d}{2k} \max \left\{ \overline{W}_d + \frac{\mu_d^{\text{eff}}}{2k} - \varepsilon, 0 \right\} \right). \quad (100)$$

Note that, by construction of Φ_d ,

$$\Phi_d(\zeta) \geq \zeta, \quad \forall \zeta \in \mathbb{R}.$$

Then, due to $W_d(s_\kappa) \leq \overline{W}_d$ and $1 + e^{z_d(s_\kappa)} > 1$, (99) implies, for all $t \in J_\kappa$,

$$z_d(t) \leq \Phi_d(z_d(s_\kappa)). \quad (101)$$

We now bound $z_d(s_0)$ at the beginning of the first OFF interval.

There are two cases: (i) $\eta(0) \geq 0$. Then $0 \in \mathcal{I}_{\text{off}}$ and hence $s_0 = 0$. In this case,

$$z_d(s_0) = z_d(0). \quad (102)$$

(ii) $\eta(0) < 0$. Then $0 \notin \mathcal{I}_{\text{off}}$, so $s_0 > 0$, and we have $[0, s_0] \subseteq \mathcal{I}_{\text{on}}$. Using (19),(96),(97), we obtain

$$\begin{aligned} z_d(s_0) - z_d(0) &= \int_0^{s_0} \dot{z}_d(s) ds \\ &\leq \int_{\mathcal{I}_{\text{on}}} \dot{z}_d(s) ds \leq \Delta z_d^{\text{on}}, \end{aligned}$$

and thus

$$z_d(s_0) \leq z_d(0) + \Delta z_d^{\text{on}}. \quad (103)$$

Combining (102) and (103), and due to $\Delta z_d^{\text{on}} \geq 0$, we obtain, in both cases,

$$z_d(s_0) \leq \max \{ z_d(0), z_d(0) + \Delta z_d^{\text{on}} \} = z_d(0) + \Delta z_d^{\text{on}}. \quad (104)$$

Since $\Phi_d(\zeta) \geq \zeta$, (104) implies

$$z_d(s_0) \leq \Phi_d(z_d(0)) + \Delta z_d^{\text{on}}. \quad (105)$$

We next proceed by defining

$$\Psi_d(\zeta) := \Phi_d(\zeta) + \Delta z_d^{\text{on}}, \quad (106)$$

which is a continuous, non-decreasing map $\Psi_d : \mathbb{R} \rightarrow \mathbb{R}$, because Φ_d is non-decreasing in ζ and Δz_d^{on} is constant. For $n \in \mathbb{N}$, we denote by $\Psi_d^{(n)}$ the n -fold composition of Ψ_d with itself and set $\Psi_d^{(1)}(\zeta) := \Psi_d(\zeta)$.

We now show by induction on κ that

$$z_d(s_\kappa) \leq \Psi_d^{(\kappa+1)}(z_d(0)), \quad \kappa = 0, 1, \dots, N_{\text{off}}. \quad (107)$$

For $\kappa = 0$, (105) gives

$$z_d(s_0) \leq \Phi_d(z_d(0)) + \Delta z_d^{\text{on}} = \Psi_d(z_d(0)) = \Psi_d^{(1)}(z_d(0)),$$

so (107) holds for $\kappa = 0$. Assume that (107) holds for some $\kappa \in \{0, \dots, N_{\text{off}} - 1\}$. We show it for $\kappa + 1$.

Between t_κ and $s_{\kappa+1}$ the filter is ON whenever $t_\kappa < s_{\kappa+1}$, so

$$z_d(s_{\kappa+1}) - z_d(t_\kappa) = \int_{t_\kappa}^{s_{\kappa+1}} \dot{z}_d(s) ds \leq \int_{\mathcal{I}_{\text{on}}} \dot{z}_d(s) ds \leq \Delta z_d^{\text{on}},$$

and

$$z_d(s_{\kappa+1}) \leq z_d(t_\kappa) + \Delta z_d^{\text{on}}. \quad (108)$$

If $t_\kappa = s_{\kappa+1}$, then the integral above is zero and $z_d(s_{\kappa+1}) = z_d(t_\kappa)$, so (108) holds trivially. On the OFF interval $J_\kappa = [s_\kappa, t_\kappa]$, we have from (101) that

$$z_d(t_\kappa) \leq \Phi_d(z_d(s_\kappa)).$$

Combining this with (108) and recalling (106) gives

$$z_d(s_{\kappa+1}) \leq \Phi_d(z_d(s_\kappa)) + \Delta z_d^{\text{on}} = \Psi_d(z_d(s_\kappa)).$$

Using the induction hypothesis (107) for κ and the monotonicity of Ψ_d , we obtain

$$z_d(s_{\kappa+1}) \leq \Psi_d \left(\Psi_d^{(\kappa+1)}(z_d(0)) \right) = \Psi_d^{(\kappa+2)}(z_d(0)),$$

which proves (107) for $\kappa + 1$. By induction, (107) holds for all $\kappa = 0, 1, \dots, N_{\text{off}}$.

In particular, for $\kappa = N_{\text{off}}$, we have

$$z_d(s_{N_{\text{off}}}) \leq \Psi_d^{(N_{\text{off}}+1)}(z_d(0)). \quad (109)$$

We now use the fact that the last OFF interval $[s_{N_{\text{off}}}, +\infty)$ is unbounded on the right and contained in \mathcal{I}_{off} (see Remark 4). On $[s_{N_{\text{off}}}, +\infty)$ the safety filter is never ON, so the controller coincides with the DADS-BS controller for all $t \geq s_{N_{\text{off}}}$. Therefore, similar to (101), we obtain using Lemma 2

$$z_d(t) \leq \Phi_d(z_d(s_{N_{\text{off}}})) \quad \forall t \geq s_{N_{\text{off}}}. \quad (110)$$

Combining (109) and (110), and using the monotonicity of Φ_d , we obtain

$$z_d(t) \leq \Phi_d \left(\Psi_d^{(N_{\text{off}}+1)}(z_d(0)) \right), \quad \forall t \geq s_{N_{\text{off}}}. \quad (111)$$

Finally, since $\dot{z}_d(t) \geq 0$, the function $z_d(\cdot)$ is non-decreasing. In particular, for any $t \in [0, s_{N_{\text{off}}}]$,

$$z_d(t) \leq z_d(s_{N_{\text{off}}}) \leq \Phi_d \left(\Psi_d^{(N_{\text{off}}+1)}(z_d(0)) \right),$$

where we used $\Phi_d(\zeta) \geq \zeta$ and (109). Therefore, (111) actually holds for all $t \geq 0$:

$$z_d(t) \leq \Phi_d \left(\Psi_d^{(N_{\text{off}}+1)}(z_d(0)) \right).$$

From (98) we have $N_{\text{off}} + 1 \leq N_\Omega + 1$. Furthermore, we have that $\Psi_d^{(\kappa_1)}(\zeta) \leq \Psi_d^{(\kappa_2)}(\zeta)$ for $\kappa_2 > \kappa_1$ and all $\zeta \in \mathbb{R}$ (this can be shown using (106) and recalling $\Phi_d(\zeta) \geq \zeta$ for all $\zeta \in \mathbb{R}$ and $\Delta z_d^{\text{on}} \geq 0$). Hence

$$\Psi_d^{(N_{\text{off}}+1)}(z_d(0)) \leq \Psi_d^{(N_\Omega+1)}(z_d(0)),$$

and, by the monotonicity of Φ_d ,

$$z_d(t) \leq \Phi_d \left(\Psi_d^{(N_\Omega+1)}(z_d(0)) \right), \quad (112)$$

for all $t \geq 0$. Since $z_d(t) \geq z_d(0)$ and z_d is non-decreasing and bounded from above by the right-hand side of (112), the limit $\lim_{t \rightarrow \infty} z_d(t)$ exists and is finite, and

satisfies the same upper bound. Recalling Φ_d and Ψ_d are given by (100) and (106), respectively, and that Δz_d^{on} depends on $\mathbf{x}(0)$, $z_d(0)$, $\|v_{g,d}\|_\infty$, $\|v_{g,q}\|_\infty$, T_Ω , we conclude that the right-hand side of (112) takes the form of a function $B_{d,\Omega}(\mathbf{x}(0), z_d(0), \|v_{g,d}\|_\infty, \|v_{g,q}\|_\infty, N_\Omega, T_\Omega)$.

An analogous analysis for z_q can be carried out in the same way. This completes the proof of Theorem 5. \square

VII. CONCLUSIONS

This paper proposed a nonlinear droop-based grid-forming (GFM) controller, by integrating a backstepping (BS) inner-outer architecture with the deadzone-adapted disturbance suppression (DADS) framework. No knowledge of network parameters beyond the point of common coupling (PCC) is required, and the grid voltage is treated as an unknown but bounded disturbance of arbitrarily large magnitude. The controller guarantees global well-posedness and boundedness of all closed-loop states (Theorem 1) and PCC voltage-formation performance with assignable residual bounds (Theorem 2). Hard over-current protection is enforced via a minimally invasive control-barrier-function-based safety filter with a closed-form solution. The safety filter is applicable to any locally Lipschitz nominal controller, including DADS-BS, and ensures forward invariance of the safe-current set and boundedness of all physical states (Theorem 4), as well as boundedness of the adaptive states in DADS-BS under mild activation assumptions (Theorem 5). Numerical results illustrate improved transient performance and faster recovery during current-limiting events when DADS-BS is used as the nominal controller, compared with conventional PI-based GFM control.

REFERENCES

- [1] D. B. Rathnayake, M. Akrami, C. Phurailatpam, S. P. Me, S. Hadavi, G. Jayasinghe, S. Zabihi, and B. Bahrani, "Grid forming inverter modeling, control, and applications," *IEEE Access*, vol. 9, pp. 114 781–114 807, 2021.
- [2] F. Milano, F. Dörfler, G. Hug, D. J. Hill, and G. Verbič, "Foundations and challenges of low-inertia systems," in *2018 Power Systems Computation Conference (PSCC)*. IEEE, 2018, pp. 1–25.
- [3] N. Baeckeland, D. Chatterjee, M. Lu, B. Johnson, and G.-S. Seo, "Overcurrent limiting in grid-forming inverters: A comprehensive review and discussion," *IEEE Transactions on Power Electronics*, vol. 39, no. 11, pp. 14 493 – 14 517, 2024.
- [4] S. Chatterjee and S. Geng, "Sensitivity to hopf bifurcation in grid-following inverters using normal vector methods," in *2024 60th Annual Allerton Conference on Communication, Control, and Computing*. IEEE, 2024, pp. 01–08.
- [5] —, "Effects of line dynamics on the stability margin to hopf bifurcation in grid-forming inverters," *Sustainable Energy, Grids and Networks*, p. 101947, 2025.
- [6] Y. Lin, J. H. Eto, B. B. Johnson, J. D. Flicker, R. H. Lasseter, H. N. Villegas Pico, G.-S. Seo, B. J. Pierre, and A. Ellis, "Research roadmap on grid-forming inverters," National Renewable Energy Lab.(NREL), Golden, CO (United States), Tech. Rep., 2020.
- [7] U. B. Tayab, M. A. B. Roslan, L. J. Hwai, and M. Kashif, "A review of droop control techniques for microgrid," *Renewable and Sustainable Energy Reviews*, vol. 76, pp. 717–727, 2017.
- [8] S. Geng and I. A. Hiskens, "Unified grid-forming/following inverter control," *IEEE Open Access Journal of Power and Energy*, vol. 9, pp. 489–500, 2022.
- [9] H.-P. Beck and R. Hesse, "Virtual synchronous machine," in *2007 9th International Conference on Electrical Power Quality and Utilisation*. IEEE, 2007, pp. 1–6.
- [10] H. Alatrash, A. Mensah, E. Mark, G. Haddad, and J. Enslin, "Generator emulation controls for photovoltaic inverters," *IEEE Transactions on Smart Grid*, vol. 3, no. 2, pp. 996–1011, 2012.
- [11] Q.-C. Zhong and G. Weiss, "Synchronverters: Inverters that mimic synchronous generators," *IEEE Transactions on Industrial Electronics*, vol. 58, no. 4, pp. 1259–1267, 2011.
- [12] B. B. Johnson, M. Sinha, N. G. Ainsworth, F. Dörfler, and S. V. Dhople, "Synthesizing virtual oscillators to control islanded inverters," *IEEE Transactions on Power Electronics*, vol. 31, no. 8, pp. 6002–6015, 2016.
- [13] M. Sinha, F. Dörfler, B. B. Johnson, and S. V. Dhople, "Uncovering droop control laws embedded within the nonlinear dynamics of van der pol oscillators," *IEEE Transactions on Control of Network Systems*, vol. 4, no. 2, pp. 347–358, 2017.
- [14] M. C. Colombino, D. Groß, J.-S. Brouillon, and F. Dörfler, "Global phase and magnitude synchronization of coupled oscillators with application to the control of grid-forming power inverters," *IEEE Transactions on Automatic Control*, vol. 64, no. 11, pp. 4496–4511, 2019.
- [15] M. Lu, S. Dutta, V. Purba, S. Dhople, and B. Johnson, "A grid-compatible virtual oscillator controller: Analysis and design," in *2019 IEEE Energy Conversion Congress and Exposition (ECCE)*. IEEE, 2019, pp. 2643–2649.
- [16] M. C. Chandorkar, D. M. Divan, and R. Adapa, "Control of parallel connected inverters in standalone AC supply systems," *IEEE Transactions on Industry Applications*, vol. 29, no. 1, pp. 136–143, 1993.
- [17] B. Fan, T. Liu, F. Zhao, H. Wu, and X. Wang, "A review of current-limiting control of grid-forming inverters under symmetrical disturbances," *IEEE Open Journal of Power Electronics*, vol. 3, pp. 955–969, 2022.
- [18] B. Mahamedi, M. Eskandari, J. E. Fletcher, and J. Zhu, "Sequence-based control strategy with current limiting for the fault ride-through of inverter-interfaced distributed generators," *IEEE Transactions on Sustainable Energy*, vol. 11, no. 1, pp. 165–174, 2020.
- [19] I. Sadeghkhani, M. E. H. Golshan, J. M. Guerrero, and A. Mehrizi-Sani, "A current limiting strategy to improve fault ride-through of inverter interfaced autonomous microgrids," *IEEE Transactions on Smart Grid*, vol. 8, no. 5, pp. 2138–2148, 2017.
- [20] N. S. Gurule, J. Hernandez-Alvidrez, M. J. Reno, A. Summers, S. Gonzalez, and J. Flicker, "Grid-forming inverter experimental testing of fault current contributions," in *2019 IEEE 46th Photovoltaic Specialists Conference (PVSC)*. IEEE, 2019, pp. 3150–3155.
- [21] T. Liu, X. Wang, F. Liu, K. Xin, and Y. Liu, "A current limiting method for single-loop voltage-magnitude controlled grid-forming converters during symmetrical faults," *IEEE Transactions on Power Electronics*, vol. 37, no. 4, pp. 4751–4763, 2022.
- [22] A. D. Paquette and D. M. Divan, "Virtual impedance current limiting for inverters in microgrids with synchronous generators," *IEEE Transactions on Industry Applications*, vol. 51, no. 2, pp. 1630–1638, 2015.
- [23] X. Wang, Y. W. Li, F. Blaabjerg, and P. C. Loh, "Virtual-impedance-based control for voltage-source and current-source converters," *IEEE Transactions on Power Electronics*, vol. 30, no. 12, pp. 7019–7037, 2015.
- [24] T. Erckrath, P. Unruh, and M. Jung, "Voltage phasor based current limiting for grid-forming converters," in *2022 IEEE Energy Conversion Congress and Exposition (ECCE)*. IEEE, 2022, pp. 1–8.
- [25] J. Chen, F. Prystupczuk, and T. O'Donnell, "Use of voltage limits for current limitations in grid-forming converters," *CSEE Journal of Power and Energy Systems*, vol. 6, no. 2, pp. 259–269, 2020.
- [26] M. A. Desai, X. He, L. Huang, and F. Dörfler, "Saturation-informed current-limiting control for grid-forming converters," *Electric Power Systems Research*, vol. 234, p. 110746, 2024.
- [27] D. Groß, "Constraint-aware grid-forming control for current limiting," *arXiv preprint arXiv:2512.00644*, 2025.
- [28] A. D. Ames, X. Xu, J. W. Grizzle, and P. Tabuada, "Control barrier function based quadratic programs for safety critical systems," *IEEE Transactions on Automatic Control*, vol. 62, no. 8, pp. 3861–3876, 2017.
- [29] S. Kundu, S. Geng, S. P. Nandanoori, I. A. Hiskens, and K. Kalsi, "Distributed barrier certificates for safe operation of inverter-based microgrids," in *2019 American Control Conference (ACC)*. IEEE, 2019, pp. 1042–1047.
- [30] M. Schneeberger, S. Mastellone, and F. Dörfler, "Safety filter for limiting the current of grid-forming matrix modular multilevel converters," *arXiv preprint arXiv:2503.10498*, 2025.
- [31] T. Joswig-Jones and B. Zhang, "Safe control of grid-interfacing inverters with current magnitude limits," *arXiv preprint arXiv:2409.13890*, 2024.
- [32] A. Tayyebi, A. Anta, and F. Dörfler, "Grid-forming hybrid angle control and almost global stability of the DC-AC power converter," *IEEE Transactions on Automatic Control*, vol. 68, no. 7, pp. 3842–3857, 2023.
- [33] L. Karunaratne, N. R. Chaudhuri, A. Yogarathnam, and M. Yue, "Nonlinear backstepping control of grid-forming converters in presence of grid-

- following converters and synchronous generators,” *IEEE Transactions on Power Systems*, vol. 39, no. 1, pp. 1948–1964, 2024.
- [34] L. F. N. Lourenco, A. Iovine, G. Damm, and A. J. Sguarezi Filho, “Nonlinear controller for MMC-HVdc operating in grid-forming mode,” *IEEE Transactions on Control Systems Technology*, vol. 33, no. 1, pp. 229 – 244, 2025.
- [35] S. K. Panda and B. Subudhi, “An extended state observer based adaptive backstepping controller for microgrid,” *IEEE Transactions on Smart Grid*, vol. 15, no. 1, pp. 171–178, 2024.
- [36] I. Karafyllis and M. Krstic, “Deadzone-adapted disturbance suppression control for global practical IOS and zero asymptotic gain to matched uncertainties,” *Systems & Control Letters*, vol. 185, p. 105746, 2024.
- [37] I. Karafyllis, M. Krstic, and A. Aslanidis, “Deadzone-adapted disturbance suppression control for strict-feedback systems,” *Automatica*, vol. 171, p. 111986, 2025.
- [38] I. Karafyllis and M. Krstic, *Robust Adaptive Control: Deadzone-Adapted Disturbance Suppression*. SIAM, 2025.
- [39] J. Schiffer, D. Zonetti, R. Ortega, A. M. Stanković, T. Sezi, and J. Raisch, “A survey on modeling of microgrids—from fundamental physics to phasors and voltage sources,” *Automatica*, vol. 74, pp. 135–150, 2016.